SIAM J. NUMER. ANAL.
Vol. 47, No. 4, pp. 2612–2637

CONVERGENCE ANALYSIS OF THE MIMETIC FINITE DIFFERENCE METHOD FOR ELLIPTIC PROBLEMS*

ANDREA CANGIANI†, GIANMARCO MANZINI‡, AND ALESSANDRO RUSSO§

Abstract. We propose a family of mimetic discretization schemes for elliptic problems including convection and reaction terms. Our approach is an extension of the mimetic methodology for purely diffusive problems on unstructured polygonal and polyhedral meshes. The a priori error analysis relies on the connection between the mimetic formulation and the lowest order Raviart–Thomas mixed finite element method. The theoretical results are confirmed by numerical experiments.

Key words. mimetic finite difference method, boundary value problem, diffusion-convection-reaction equation, Raviart–Thomas finite element space, dual mixed formulation, polyhedral mesh

AMS subject classifications. 65N06, 65N12, 65N15, 65N22, 65N30

DOI. 10.1137/080717560

1. Introduction.

We consider the steady convection-diffusion-reaction problem

$$-\mathrm{div}\,(K\nabla p + \boldsymbol{b}p) + cp = f \qquad \text{in } \Omega, \tag{1.1a}$$

$$p = g \qquad \text{on } \Gamma \tag{1.1b}$$

for the scalar solution field p defined on the domain $\Omega \subset \mathbb{R}^d$, $d = 2, 3$, with boundary Γ. The functions f and g are, respectively, the source term and the boundary data, K is a full symmetric tensor describing material properties, $\boldsymbol{b}$ is the convection field, and c is the reaction field.

The accurate and stable solution of diffusion problems involving convection and reaction terms is a challenging task and one of fundamental importance in the field of numerical solution of partial differential equations. All classical numerical methods, e.g., finite differences, finite elements, and finite volumes, have been studied extensively, in particular concerning the numerical treatment of (1.1) in the convection- and reaction-dominated regimes [40, 41].

In this work, we extend the family of mimetic finite difference (MFD) methods introduced in [12, 14] for purely diffusive problems to include the convection and reaction terms. The MFD method interest and strength is in the superior flexibility allowed in the mesh design which can be particularly useful in the presence of heterogeneous materials (e.g., oil reservoir) and if we require mesh adaptivity.

We focus on the mixed form of (1.1) (see section 2) and perform the a priori analysis in the diffusive regime. Our analysis exploits the strong similarities that the mimetic finite difference method shows with the lowest order mixed finite element method analyzed by Douglas and Roberts in [21, 22]; see also [42]. Apparently,

*Received by the editors March 4, 2008; accepted for publication (in revised form) March 6, 2009; published electronically July 22, 2009.
http://www.siam.org/journals/sinum/47-4/71756.html

†Dipartimento di Matematica e Applicazioni, Università degli Studi di Milano Bicocca, via R. Cozzi 53, Edificio U5, I-20125 Milano, Italy (andrea.cangiani@unimib.it). This author's research was partially supported by the European Project *CardioWorkBench - Drug Design for Cardiovascular Diseases*.

‡Istituto di Matematica Applicata e Tecnologie Informatiche (IMATI) – CNR, via Ferrata 1, I – 27100 Pavia, Italy (Marco.Manzini@imati.cnr.it).

§Dipartimento di Matematica e Applicazioni, Università degli Studi di Milano Bicocca, via R. Cozzi 53, Edificio U5, I-20125 Milano, Italy (alessandro.russo@unimib.it).

the development of *stable* mixed finite element methods, suitable to the numerical resolution of convection-dominated problems, has not obtained much attention by researchers. To the best of our knowledge, the only work that follows this direction is found in [35].

Other techniques for the solution of convection-diffusion problems, which hold a close relationship with the mimetic approach, are in the framework of the finite volume methods. A review of this class of methods is found in [24]. Among the most recent developments concerning elliptic problems with convection terms we mention the discretizations based on the *two-point flux formula* [27] for noncoercive convection-diffusion equations [23]. These methods were originally formulated for meshes of simplexes. Extensions to general meshes are possible by using proper cell-based reconstructions of the solution gradient as the one proposed in [25]. An alternative finite volume formulation that is suitable for very general shaped control volumes is based on the *diamond scheme* [18, 19]. It is also worth mentioning the very recent *discrete duality finite volume methods* for linear and nonlinear purely elliptic problems [1, 20, 28, 29], which fit perfectly into the framework of mimetic discretizations and whose extension to include convection terms is in progress [17]. All these numerical schemes can be considered as discretizations of the mixed form of (1.1) provided that an explicit formula is known for the calculation of the flux variable. The mixed form of the convection-reaction equation is also the starting point for the discretization given by the local discontinuous Galerkin method reviewed in [16]. The use of *direct* discontinuous Galerkin methods, such as the interior-penalty discontinuous Galerkin finite element methods, is discussed in [30], where the case of vanishing diffusion (partial differential equations with nonnegative characteristic form) is also considered.

Although MFD methods are quite recent, there is a vast amount of literature concerning their application to purely diffusive problems; see, e.g., [5, 6, 31, 32, 33, 38, 39] and the more recent works [2, 3, 4, 8, 11, 12, 13, 14, 15, 26, 34, 36, 37]. The rapid growth of interest in mimetic methodologies is due to the great flexibility allowed in the mesh design. Starting from [38] dealing with hexahedral elements, we witness the development of mimetic discretizations on unstructured polygonal and polyhedral meshes in [34, 36], subsequently improved and generalized in [11, 12, 13, 14]. The a priori analysis of MFD methods on polyhedral meshes including nonconvex and degenerate elements is carried out by Brezzi, Lipnikov, and Shashkov in [12] and extended by the same authors to generalized polyhedral elements with curved faces in [13]. The computational aspects are considered in [11, 14] where it is shown how to construct a family of inexpensive mimetic schemes.

The method presented here is built over the MFD family developed in [12, 14]. We use the same assumptions on the diffusion tensor (strong ellipticity), mesh shape-regularity, and mimetic scalar products introduced in the aforementioned paper and the same discretization of the diffusion term. Our a priori analysis exploits the connection between the MFD method and the mixed finite element discretizations: an MFD method can be analyzed as a finite element method if there exists a lifting operator acting on the degrees of freedom of the vector variable. We emphasize that the existence of the lifting operator is assumed only to analyze the method. In fact, the implementation proposed in [14], which is the basis of this work, does not require the explicit knowledge of the lifting operator. Numerical experiments show that the predicted convergence rates are attained anyway.

Technically, we follow the analysis of the mixed finite element method for general second order elliptic equations proposed by Douglas and Roberts in [21, 22], which dates back to the mid 1980s. We obtain optimal convergence estimates for the scalar

solution field in the L^2-norm and the flux in a modified $H(\mathsf{div})$-norm. Moreover, we prove the superconvergence of the solution's elemental averages in analogy to the estimates for diffusion problems proved in [12]. This could be exploited to postprocess a higher order approximation of the solution in much the same way as in [15].

The asymptotic convergence rates will not be observed when the convection and reaction terms dominate and the mesh is not fine enough to solve the solution layers. The setup of stabilized MFD methods is beyond the scope of the present paper and will be the topic of future work.

The outline of the paper is as follows. In section 2 we describe the mimetic finite difference method focusing on the discretization of the convection and reaction terms. In section 3 we develop the a priori analysis of the method deriving error estimates for scalar solution and flux. In section 4 we present some numerical results that confirm the theoretical estimates on unstructured meshes comprising convex and nonconvex elements. Finally, in section 5 we draw some final remarks and conclusions.

2. Mimetic finite difference formulation.

2.1. Mixed variational formulation. Let Ω be a polyhedral domain for $d = 3$ (polygonal for $d = 2$) with Lipschitz continuous boundary Γ. We reformulate the model problem (1.1) in mixed form by introducing the vector field $\boldsymbol{F}$ representing the *flux*:

$$\boldsymbol{F} = -\left(K\nabla p + \boldsymbol{b}p\right) \qquad \text{in } \Omega, \tag{2.1a}$$

$$\mathrm{div}\boldsymbol{F} + cp = f \qquad \text{in } \Omega, \tag{2.1b}$$

$$p = g \qquad \text{on } \Gamma. \tag{2.1c}$$

We set the problem in the functional spaces

$$V := \left\{ \boldsymbol{v} \in \left(L^2(\Omega)\right)^d \text{ such that } \mathrm{div}\boldsymbol{v} \in L^2(\Omega) \right\} = H(\mathsf{div}, \Omega),$$
$$W := L^2(\Omega).$$

The space V is a Hilbert space when equipped with the scalar product

$$(\boldsymbol{v}, \boldsymbol{u})_{H(\mathsf{div},\Omega)} = \int_\Omega \boldsymbol{v} \cdot \boldsymbol{u}\, dV + \int_\Omega \mathrm{div}\boldsymbol{v}\, \mathrm{div}\boldsymbol{u}\, dV$$

and the corresponding norm

$$\|\boldsymbol{v}\|^2_{H(\mathsf{div},\Omega)} = \|\boldsymbol{v}\|^2_{L^2(\Omega)} + \|\mathrm{div}\boldsymbol{v}\|^2_{L^2(\Omega)}.$$

The *mixed variational formulation* of problem (2.1) reads as follows [10]: *find* $(\boldsymbol{F}, p) \in V \times W$ *such that*

$$(\alpha\boldsymbol{F}, \boldsymbol{v}) - (p, \mathrm{div}\boldsymbol{v}) + (\alpha\boldsymbol{b}p, \boldsymbol{v}) = \langle g, \boldsymbol{n}\cdot\boldsymbol{v}\rangle \qquad \forall \boldsymbol{v} \in V, \tag{2.2a}$$

$$(\mathrm{div}\boldsymbol{F}, w) + (cp, w) = (f, w) \qquad \forall w \in W, \tag{2.2b}$$

where

$$\langle g, \boldsymbol{n}\cdot\boldsymbol{v}\rangle := \sum_{e\subset\Gamma} \int_e g\boldsymbol{n}^e \cdot \boldsymbol{v}\, dS,$$

and $\boldsymbol{n}_e$ represents the unit normal to the boundary face $e \subset \Gamma$ pointing out of the polyhedral domain Ω.

Problem (1.1) is well-posed and admits a unique solution under the following hypothesis:

(H) $f \in L^2(\Omega)$, $g \in H^{1/2}(\Gamma)$, K *strongly elliptic* with the components in $L^\infty(\Omega)$, $\boldsymbol{b} \in (W^{1,\infty}(\Omega))^d$, and $c \in W^{1,\infty}(\Omega)$ and satisfying $-(1/2)\mathrm{div}\boldsymbol{b} + c \geq 0$ almost everywhere in Ω.

We recall that the tensor field K is strongly elliptic if there exist two positive constants κ_* and κ^* such that

$$\kappa_* \|\boldsymbol{G}\|^2 \leq \boldsymbol{G}^T K \boldsymbol{G} \leq \kappa^* \|\boldsymbol{G}\|^2 \qquad \forall \boldsymbol{G} \in \mathbb{R}^d.$$

2.2. Notation and basic assumptions. The formulation of mimetic finite difference methods is based on the notion of *discrete fields*. These are collections of real numbers representing the degrees of freedom of the numerical scheme. To ease notation, we do not make any explicit distinction between continuous and discrete fields, as their nature can be contextually derived without ambiguity, and we reserve bold letters to indicate *vector fields*.

Let $\mathcal{T}_h$ be a conformal partition of Ω into nonoverlapping polyhedral elements (polygons in two dimensions). For every element E we denote its d-dimensional Lebesgue measure by $|E|$, its diameter by h_E, and the number of its faces by m_E. Similarly, for every face e we denote its $(d-1)$-dimensional Lebesgue measure by $|e|$, the number of its edges by m_e, and the $(d-2)$ measure of the edge l by $|l|$. The notation ∂E may denote the boundary of the element E or the union of the element faces depending on the context. We also set, as usual, $h = \sup_E h_E$.

We make the following assumption on the diffusion field:

(K) all components K and its inverse $\alpha = K^{-1}$ together with their first derivatives are locally bounded functions; i.e., for every $E \in \mathcal{T}_h$ and $i, j = 1, \ldots d$, we assume that $K_{i,j}|_E$ and $\alpha_{i,j}|_E$ are in $W^{1,\infty}(E)$ and

$$\|K\|_{W^{1,\infty}(E)} = \max_{i,j} \|K_{ij}\|_{W^{1,\infty}(E)} \leq C_K,$$
$$\|\alpha\|_{W^{1,\infty}(E)} = \max_{i,j} \|\alpha_{ij}\|_{W^{1,\infty}(E)} \leq C_\alpha,$$

with constants C_K and C_α independent of E.

From the above assumption it follows that there exists a tensor $\widetilde{\alpha}$ piecewise constant on $\mathcal{T}_h$ whose restriction $\widetilde{\alpha}_E$ to each element $E \in \mathcal{T}_h$ is a nonsingular matrix which gives an approximation of order $\mathcal{O}(h_E)$ of $\alpha|_E$; formally,

$$\max_{i,j} \|\widetilde{\alpha}_{ij}|_E - \alpha_{ij}\|_{L^\infty(E)} \leq \widetilde{C}_\alpha h_E, \tag{2.3}$$

where the constant $\widetilde{C}_\alpha$ is independent of E.

Since this work is set in the framework of references [12, 14], we consider the mesh regularity assumptions of these works. These assumptions are formulated for $d = 3$; the restriction to $d = 2$ is straightforward. In what follows, "$a \approx b$" indicates that the left-hand side a is uniformly bounded from above and from below by the right-hand side b.

(M1) There exist two positive integers N_e and N_l such that every element E has $m_E \leq N_e$ faces, and every face e has $m_e \leq N_l$ edges.

(M2) For every edge l of every element E, it holds $|l| \approx h_E$.

(M3) There exists a positive number τ^* such that each element E is star-shaped with respect to all points of a ball of radius $\tau^* h_E$ and center at a point $M_E \in E$.

(M4) There exists a positive number γ^* such that each face $e \in \partial E$ is star-shaped with respect to all points of a ball of radius $\gamma^* h_E$ and center at a point $M_e \in e$.

(M5) For every element E and for every face $e \in \partial E$ there exists a pyramid contained in E and having base coincident with e, height equal to $\gamma^* h_E$, and such that the projection of its vertex onto e is M_e.

Note that (M1) is a "structural" assumption on the shape of elements and faces, and (M1)–(M2) imply both scalings $|E| \approx h_E^d$ and $|e| \approx h_E^{(d-1)}$. Assumptions (M3)–(M5) are not directly exploited in this paper, but they are fundamental to derive the approximation properties of the lifting operator (cf. subsection 3.1) and the a priori estimates for the pure elliptic case [12]. We listed them above for completeness of exposition.

2.3. Scheme formulation. We start by defining two linear spaces of discrete fields, which are denoted by Q_h and X_h, representing the degrees-of-freedom for the scalar variable and the flux. We associate the degrees-of-freedom of the scalar variable to mesh cells so that

$$\text{for } \; q \in Q_h, \quad q = \{q_E\}_{E\in\mathcal{T}_h} \; \text{ with } \; q_E \in \mathbb{R}.$$

Flux degrees-of-freedom are associated with mesh faces so that

$$\text{for } \; \boldsymbol{G} \in X_h, \quad \boldsymbol{G} = \{G_E^e\}_{E\in\mathcal{T}_h}^{e\in\partial E} \; \text{ with } \; G_E^e \in \mathbb{R},$$

with the additional assumption of normal flux continuity:

$$G_{E_1}^e + G_{E_2}^e = 0 \; \text{ when } \; e \in E_1 \cap E_2, \quad E_1,\, E_2 \in \mathcal{T}_h.$$

In view of the previous definitions, the dimension of Q_h equals the number of mesh cells and the dimension of X_h equals the number of mesh faces. We also introduce two interpolation operators for, respectively, $q \in L^1(\Omega)$ and $\boldsymbol{G} \in (L^s(\Omega))^d$ with $s > 2$ and $\mathrm{div}\boldsymbol{G} \in L^2(\Omega)$ as

$$\begin{aligned}
\big(q^I\big)_E &= \frac{1}{|E|}\int_E q\, dV \quad \text{for all } E \in \mathcal{T}_h,\\
\Big(\boldsymbol{G}^I\Big)_E^e &= \frac{1}{|e|}\int_e \boldsymbol{n}_E^e \cdot \boldsymbol{G}\, dS \quad \text{for all } e \in \partial E,\, E \in \mathcal{T}_h
\end{aligned}$$

and denote the restriction of $\boldsymbol{G}^I \in X_h$ to the faces of ∂E by $\boldsymbol{G}_E^I = \{(\boldsymbol{G}^I)_E^e\}^{e\in\partial E}$.

We equip Q_h and X_h with two suitable scalar products. We define the scalar product in Q_h as

$$[p,q]_{Q_h} = \sum_{E\in\mathcal{T}_h} |E| p_E q_E \;\; \text{for all } p, q \in Q_h,$$

which corresponds to the L^2-scalar product for piecewise constant functions. The scalar product is defined in X_h by assembling the elementwise contribution from each mesh element E:

$$[\boldsymbol{F},\boldsymbol{G}]_{X_h} = \sum_{E\in\mathcal{T}_h} [\boldsymbol{F},\boldsymbol{G}]_E \;\; \text{for all } \boldsymbol{F},\boldsymbol{G} \in X_h.$$

The *local* scalar product $[\cdot,\cdot]_E$ on $X_h|_E$ is required to satisfy the two following conditions:

- (S1) *stability*: there exist two constants C_*, $C^* > 0$ independent of h such that

$$C_* \sum_{e\in\partial E} |E| \left(\boldsymbol{G}_E^e\right)^2 \le [\boldsymbol{G},\boldsymbol{G}]_E \le C^* \sum_{e\in\partial E} |E| \left(\boldsymbol{G}_E^e\right)^2$$

for all $\boldsymbol{G} \in X_h$ and for every element E;

- (S2) *local consistency*: for every linear function q^1 on $E \in \mathcal{T}_h$

$$\left[\left(\widetilde{K}\nabla q^1\right)^I, \boldsymbol{G}\right]_E + \int_E q^1 \mathcal{DIV}_h \boldsymbol{G}\, dV = \sum_{e\in\partial E} \boldsymbol{G}_E^e \int_e q^1\, dS$$

for all $\boldsymbol{G} \in X_h$.

The local scalar product is specified through an $m_E \times m_E$ symmetric and positive definite matrix M_E:

$$[\boldsymbol{F},\boldsymbol{G}]_E = \boldsymbol{F}_E^T M_E \boldsymbol{G}_E,$$

where $\boldsymbol{F}_E$ and $\boldsymbol{G}_E$ are the vectors formed by the components of $\boldsymbol{F}$ and $\boldsymbol{G}$ related to the faces $e \in \partial E$. The convergence properties of the MFD method presented here depend only on the fact that the local scalar product satisfies assumptions (S1)–(S2) and not on the specific form of the matrix M_E. Details on the particular choice of the matrix M_E used in the numerical experiments are given in section 4. The symbols $\|\!|\cdot|\!\|_{Q_h}$, $|\!|\!|\cdot|\!|\!|_{X_h}$, and $|\!|\!|\cdot|\!|\!|_E$ will be used to denote the norms induced by the scalar products defined above.

The mimetic *discrete divergence* operator $\mathcal{DIV}_h : X_h \to Q_h$ is defined elementwise as

$$\left(\mathcal{DIV}_h \boldsymbol{G}\right)_E = \frac{1}{|E|} \sum_{e\in\partial E} |e| \boldsymbol{G}_E^e \quad \text{for } \boldsymbol{G} \in X_h \quad \text{for } E \in \mathcal{T}_h.$$

This definition is consistent with the Gauss divergence theorem. Furthermore, from the definition of the interpolation operators it easily follows that

$$(\mathrm{div}\boldsymbol{G})^I = \mathcal{DIV}_h \boldsymbol{G}^I.$$

All the definitions introduced so far are in accordance with references [12, 14] and are all that is needed to discretize pure diffusive problems.

For the discretization of the convection and reaction terms we proceed as follows. We replace all continuous data α, $\boldsymbol{b}$, and c by their interpolants $\widetilde{\alpha}$, $\boldsymbol{b}^I$, and c^I, respectively, and the solution field p and flux field $\boldsymbol{F}$ with the corresponding mimetic fields p_h and $\boldsymbol{F}_h$. Using the scalar product $[\cdot,\cdot]_E$ in place of the L^2 product we obtain the discrete form of the convection term in (2.2a):

$$\int_\Omega \alpha \boldsymbol{b} p \cdot \boldsymbol{v}\, dV = \sum_{E\in\mathcal{T}_h} \int_E \alpha \boldsymbol{b} p \cdot \boldsymbol{v}\, dV \quad \longrightarrow \quad \sum_{E\in\mathcal{T}_h} p_E \left[\boldsymbol{b}^I, \boldsymbol{G}\right]_E,$$

where the test function $\boldsymbol{v} \in V$ is replaced by $\boldsymbol{G} \in X_h$. Notice that the discrete convection term cannot be written in terms of the global scalar product operating in X_h as p_E is discontinuous on elemental faces. Similarly, we obtain the discrete form of the reaction term in (2.2b):

$$(cp, w) = \sum_{E\in\mathcal{T}_h} \int_E cpw\, dV \quad \longrightarrow \quad \sum_{E\in\mathcal{T}_h} |E| \left(c^I\right)_E p_E q_E = \left[c^I p_h, q\right]_{Q_h},$$

where $w \in W$ and $q \in Q_h$.

By using (2.5) we obtain the following discrete variational formulation: *find* $(\boldsymbol{F}_h, p_h) \in X_h \times Q_h$ *such that*

$$[\boldsymbol{F}_h, \boldsymbol{G}]_{X_h} - [p_h, \mathcal{DIV}_h \boldsymbol{G}]_{Q_h} + \sum_{E\in\mathcal{T}_h} p_E \left[\boldsymbol{b}^I, \boldsymbol{G}\right]_E = \sum_{e\subset\Gamma} |e| G_E^e \bar{g}^e \ \forall \boldsymbol{G} \in X_h, \tag{2.4a}$$

$$[\mathcal{DIV}_h \boldsymbol{F}_h, q]_{Q_h} + \left[c^I p_h, q\right]_{Q_h} = \left[f^I, q\right]_{Q_h} \ \forall q \in Q_h. \tag{2.4b}$$

The Dirichlet boundary condition (1.1b) is expressed in the right-hand side of (2.4a) through interpolation of the boundary data, i.e., by defining for each boundary edge $e \subset \Gamma$:

$$\bar{g}^e = \frac{1}{|e|} \int_e g \, dS.$$

Remark 2.1. We emphasize that the numerical setting of (2.4) does not require an explicit definition of a discrete flux operator. However, this operator can be defined as the adjoint of the discrete divergence operator. To this end, we introduce the space δQ_h such that

$$\text{for} \ \ \delta q \in \delta Q_h, \quad \delta q = \{\delta q^e\}^{e\subset\Gamma} \quad \text{with} \ \ \delta q^e \in \mathbb{R},$$

which describes the "trace" of the discrete scalars on the boundary Γ. Then, we define the flux operator $\mathcal{G}_h : Q_h \times \delta Q_h \to X_h$ by

$$[\boldsymbol{G}, \mathcal{G}_h(q, \delta q)]_{X_h} = -[\mathcal{DIV}_h \boldsymbol{G}, q]_{Q_h} + \sum_{e\subset\Gamma} |e| G_E^e \delta q^e \tag{2.5}$$

for all $(q, \delta q) \in Q_h \times \delta Q_h$ and $\boldsymbol{G} \in X_h$. Equation (2.5) establishes a discrete Green-like relation with respect to the scalar products of Q_h, with X_h and $\mathcal{G}_h(q, \delta q) \in X_h$ representing the flux of the scalar field $(q, \delta q) \in Q_h \times \delta Q_h$.

An equivalent formulation more suitable for the analysis is derived by expressing the scalar product through a *lifting operator*. We consider the subset of scalar products for $X_h|_E$ satisfying (S1)–(S2) and that can be reformulated as

$$[\boldsymbol{F}, \boldsymbol{G}]_E = \int_E \widetilde{\alpha}_E R_E(\boldsymbol{F}_E) \cdot R_E(\boldsymbol{G}_E) \, dV \qquad \forall \boldsymbol{F}, \boldsymbol{G} \in X_h \tag{2.6}$$

for some *elemental lifting operator* $R_E : X_h|_E \to (L^2(E))^3$ satisfying

(L1) for all $\boldsymbol{G} \in X_h$, it holds

$$R_E(\boldsymbol{G}_E)|_e \cdot \boldsymbol{n}_e = G_E^e \qquad \forall e \in \partial E, \tag{2.7a}$$

$$\mathrm{div} R_E(\boldsymbol{G}_E) = (\mathcal{DIV}_h \boldsymbol{G})_E \qquad \text{in } E; \tag{2.7b}$$

(L2) for all constant vector fields defined on E, i.e., such that $\boldsymbol{G}_E = \boldsymbol{G}|_E =$ constant, it holds

$$R_E\left(\boldsymbol{G}_E^I\right) = \boldsymbol{G}_E.$$

In the paper we will also employ the *global lifting operator* $R : X_h \to (L^2(\Omega))^d$ built by combining the elementwise contributions from each local operator $R_E(\cdot)$. The requirement that the scalar product can be written as in (2.6) through a lifting operator satisfying (L1)–(L2) is not too restrictive; see [11] for details.

We introduce the finite dimensional functional spaces $V_h := R(X_h) \subset H(\mathsf{div}, \Omega)$ and $W_h := P_0(\mathcal{T}_h) \subset L^2(\Omega)$. Accordingly, we rewrite the scalar product in X_h as the L^2 product of the lifted fields by (2.6) and identify the scalar product for discrete scalars of Q_h with the L^2-scalar product for the corresponding piecewise constant functions in W_h. As noted above, we use the same symbols to denote scalar fields in Q_h and W_h.

By using the scalar product definition given in (2.6), we reformulate the convection term as

$$\sum_{E\in\mathcal{T}_h} p_E \left[\boldsymbol{b}^I, \boldsymbol{G}\right]_E = \sum_{E\in\mathcal{T}_h} p_E \int_E \widetilde{\alpha}_E R_E\left(\boldsymbol{b}^I\right) \cdot R_E(\boldsymbol{G})\, dV$$
$$= \int_\Omega \widetilde{\alpha} R\left(\boldsymbol{b}^I\right) p_h \cdot R(\boldsymbol{G})\, dV = \left(\widetilde{\alpha} R\left(\boldsymbol{b}^I\right) p_h, R(\boldsymbol{G})\right).$$

Finally, by noting that the equality $(f^I, w) = (f, w)$ holds for every $w \in W_h$ we arrive at the equivalent formulation: *find* $(\boldsymbol{F}_h, p_h) \in X_h \times Q_h$ *such that*

$$(\widetilde{\alpha} R(\boldsymbol{F}_h), \boldsymbol{v}) - (p_h, \mathrm{div}\boldsymbol{v}) + \left(\widetilde{\alpha} R\left(\boldsymbol{b}^I\right) p_h, \boldsymbol{v}\right) = \langle g, \boldsymbol{n}\cdot\boldsymbol{v}\rangle \ \ \forall \boldsymbol{v} \in V_h, \tag{2.8a}$$

$$(\mathrm{div} R(\boldsymbol{F}_h), w) + \left(c^I p_h, w\right) = (f, w) \ \ \forall w \in W_h. \tag{2.8b}$$

3. A priori analysis. In this section, $(\boldsymbol{F}, p) \in V \times W$ and $(\boldsymbol{F}_h, p_h) \in V_h \times W_h$, respectively, denote the exact flux and scalar solution of the dual mixed variational formulation (2.2) and discrete flux and scalar solution of the mimetic variational formulation (2.4). The symbol C will denote generic constants whose value, possibly different at any occurrence, does not depend on the mesh parameter h. The present analysis is closely related to that of finite element methods, from which we shall borrow some standard tools and techniques, e.g., the Bramble–Hilbert lemma and the interpolation error estimates. These topics can be found in several textbooks, such as, for example, [9, 10].

3.1. Error equations and orthogonality lemmas. The error equations are obtained by testing the mixed variational formulation (2.2a)–(2.2b) in the finite dimensional subspaces $V_h \times W_h$ and taking the difference with the mimetic formulation (2.8a)–(2.8b):

$$(\alpha\boldsymbol{F} - \widetilde{\alpha} R(\boldsymbol{F}_h), \boldsymbol{v}) - (p - p_h, \mathrm{div}\boldsymbol{v}) + \left(\alpha\boldsymbol{b}p - \widetilde{\alpha} R\left(\boldsymbol{b}^I\right) p_h, \boldsymbol{v}\right) = 0 \quad \forall \boldsymbol{v} \in V_h, \tag{3.1a}$$

$$(\mathrm{div}(\boldsymbol{F} - R(\boldsymbol{F}_h)), w) + \left(cp - c^I p_h, w\right) = 0 \quad \forall w \in W_h. \tag{3.1b}$$

Remark 3.1. It is possible to rewrite the divergence error equation (3.1b) in a "stronger" form. Indeed, as all terms in (2.8b) are piecewise constant functions, this is equivalent to

$$\mathrm{div} R(\boldsymbol{F}_h) + c^I p_h = f^I. \tag{3.2}$$

Subtracting (3.2) from (2.1b) yields the following error equation for the divergence of the flux:

$$\mathrm{div}(\boldsymbol{F} - R(\boldsymbol{F}_h)) + cp - c^I p_h = f - f^I, \tag{3.3}$$

which is stronger than (3.1b) as the former implies the latter. Note that an error equation in a similar stronger form cannot be derived for the flux variable.

By analogy with the analysis of mixed finite elements, we introduce the following orthogonality relations [10].

LEMMA 3.1 (orthogonality relations). *We have*

$$\left(\operatorname{div}\left(\boldsymbol{v} - R\left(\boldsymbol{v}^I\right)\right), w\right) = 0 \qquad \forall \boldsymbol{v} \in V \quad \forall w \in W_h, \tag{3.4a}$$

$$\left(\operatorname{div}\boldsymbol{v}, w - w^I\right) = 0 \qquad \forall \boldsymbol{v} \in V_h \quad \forall w \in W. \tag{3.4b}$$

Proof. As $(\operatorname{div} R(\boldsymbol{v}^I))_E = (\mathcal{DIV}_h \boldsymbol{v}^I)_E = (\operatorname{div}\boldsymbol{v})^I_E$ for every $\boldsymbol{v} \in V_h$ and $w|_E = w_E$ is constant on E for every $w \in W_h$, relation (3.4a) follows by noting that

$$\begin{aligned}\left(\operatorname{div}\left(\boldsymbol{v} - R\left(\boldsymbol{v}^I\right)\right), w\right) &= \sum_{E\in\mathcal{T}_h} \int_E \operatorname{div}\left(\boldsymbol{v} - R\left(\boldsymbol{v}^I\right)\right) w \, dV \\ &= \sum_{E\in\mathcal{T}_h} w_E \left(\int_E \operatorname{div}\boldsymbol{v}\, dV - (\operatorname{div}\boldsymbol{v})^I_E |E|\right) = 0.\end{aligned}$$

To obtain (3.4b), we note that, for every $\boldsymbol{v} \in V_h = R(X_h)$, there exists at least one discrete vector $\boldsymbol{G} \in X_h$ such that $\boldsymbol{v} = R(\boldsymbol{G})$. As $(\operatorname{div} R(\boldsymbol{G}))_E = (\mathcal{DIV}_h(\boldsymbol{G}))_E$ is constant on E we have

$$\begin{aligned}\left(\operatorname{div}\boldsymbol{v}, w - w^I\right) &= \sum_{E\in\mathcal{T}_h} \int_E (\operatorname{div} R(\boldsymbol{G}))_E \left(w - w^I\right) \, dV \\ &= \sum_{E\in\mathcal{T}_h} (\mathcal{DIV}_h \boldsymbol{G})_E \left(\int_E w \, dV - \left(w^I\right)_E |E|\right) = 0. \qquad \square\end{aligned}$$

Let us state some useful interpolation error estimates.

LEMMA 3.2. *Let R be the global lifting operator defined in the previous section satisfying* (L1)–(L2) *and* (S1)–(S2). *Under assumptions* (M1)–(M5),

$$\left\|\boldsymbol{v} - R\left(\boldsymbol{v}^I\right)\right\|_{L^2(\Omega)} \le Ch \left\|\boldsymbol{v}\right\|_{H^1(\Omega)} \qquad \forall \boldsymbol{v} \in \left(H^1(\Omega)\right)^d.$$

Proof. As shown in [13], properties (S1)–(S2) imply the local approximation result:

$$\left\|\boldsymbol{v} - R_E\left(\boldsymbol{v}^I\right)\right\|_{L^2(E)} \le Ch_E \left\|\boldsymbol{v}\right\|_{H^1(E)} \qquad \forall \boldsymbol{v} \in \left(H^1(E)\right)^d \; \forall E \in \mathcal{T}_h.$$

The lemma follows by summing the contribution of all the elements of the partition $\mathcal{T}_h$. $\square$

For future reference, we state the analogous bound in the $L^\infty(\Omega)$-norm in terms of the convective field $\boldsymbol{b}$.

LEMMA 3.3. *Let $\boldsymbol{b} \in W^{1,\infty}(\Omega)$. Under the hypothesis of Lemma* 3.2, *it holds*

$$\left\|\boldsymbol{b} - R\left(\boldsymbol{b}^I\right)\right\|_{L^\infty(\Omega)} \le Ch \|\boldsymbol{b}\|_{W^{1,\infty}(\Omega)}. \tag{3.5}$$

Proof. As $\boldsymbol{b}|_E = R_E(\boldsymbol{b}^I|_E)$ for piecewise constant vector functions, by the Bramble–Hilbert lemma we have that

$$\left\|\boldsymbol{b} - R\left(\boldsymbol{b}^I\right)\right\|_{L^\infty(E)} \le Ch \|\boldsymbol{b}\|_{W^{1,\infty}(E)} \qquad \forall E \in \mathcal{T}_h,$$

and (3.5) follows. $\square$

A similar bound holds for scalar reaction fields $c \in W^{1,\infty}(\Omega)$.

LEMMA 3.4. *Under the hypothesis of Lemma* 3.2, *we have*

$$\left\| c - c^I \right\|_{L^\infty(\Omega)} \leq Ch \|c\|_{W^{1,\infty}(\Omega)}. \tag{3.6}$$

The following lemma generalizes the well-known relation $\mathcal{DIV}_h \boldsymbol{F}^I = \mathcal{DIV}_h \boldsymbol{F}_h$, which holds when the reaction term is absent.

LEMMA 3.5. *Under the regularity assumption on c of Lemma* 3.4 *it holds*

$$\mathrm{div} R\left(\boldsymbol{F}^I - \boldsymbol{F}_h\right) + (cp)^I - c^I p_h = 0 \tag{3.7}$$

and

$$\left\| (cp)^I - c^I p_h \right\|_{L^2(\Omega)} \leq Ch \|c\|_{W^{1,\infty}(\Omega)} \|p\|_{H^1(\Omega)} + \|c\|_{L^\infty(\Omega)} \|p - p_h\|_{L^2(\Omega)}. \tag{3.8}$$

Proof. By adding and subtracting $R(\boldsymbol{F}^I)$ into the first term of second error relation (3.1b) and using the first orthogonality relation (3.4a) we get

$$\begin{aligned} 0 &= \left(\mathrm{div}\left(\boldsymbol{F} - R\left(\boldsymbol{F}^I\right)\right), w\right) + \left(\mathrm{div} R\left(\boldsymbol{F}^I - \boldsymbol{F}_h\right), w\right) + \left(cp - c^I p_h, w\right) \\ &= \left(\mathrm{div} R\left(\boldsymbol{F}^I - \boldsymbol{F}_h\right), w\right) + \left((cp)^I - c^I p_h, w\right) \end{aligned}$$

for every piecewise constant function w, and the first statement of the lemma follows. To prove inequality (3.8), we note that

$$\begin{aligned} \left\| (cp)^I - c^I p_h \right\|_{L^2(\Omega)} &\leq \left\| (cp)^I - cp \right\|_{L^2(\Omega)} + \left\| (c - c^I) p \right\|_{L^2(\Omega)} + \left\| c^I (p - p_h) \right\|_{L^2(\Omega)} \\ &\leq Ch \|c\|_{W^{1,\infty}(\Omega)} \|p\|_{H^1(\Omega)} + Ch \|c\|_{W^{1,\infty}(\Omega)} \|p\|_{L^2(\Omega)} \\ &\quad + \left\| c^I \right\|_{L^\infty(\Omega)} \|p - p_h\|_{L^2(\Omega)}, \end{aligned}$$

where we used a standard interpolation error estimate and (3.6). ∎

3.2. The duality lemmas. The a priori analysis is based on a bound of $p^I - p_h$ in the mesh-dependent norm $\|\!| \cdot |\!\|_{Q_h}$. This is achieved in the following lemma by a duality argument in analogy with the derivation of the general estimates for mixed finite elements by Douglas and Roberts [21, 22]. In the lemma, two cases are considered: in the first case we assume general K and $\boldsymbol{b}$, while in the second case we restrict K to be piecewise constant and take $\boldsymbol{b} \in V_h$. The latter setting will allow us to prove the superconvergence of p_h to p^I in the mesh-dependent norm $\|\!| \cdot |\!\|_{Q_h}$. The case $\boldsymbol{b} \in V_h$ is relevant as the convection field $\boldsymbol{b}$ may come from the numerical approximation of another partial differential equation, e.g., the Navier–Stokes equations.

The mesh-dependent error $\|\!| p^I - p_h |\!\|_{Q_h}$ is estimated as follows.

LEMMA 3.6 (duality). *Let* Ω *be a convex domain with Lipschitz continuous boundary. Under assumptions* (H)–(K), (S1)–(S2), (L1)–(L2), and (M1)–(M5) *and for h small enough it holds*

$$\left\|\!\left| p^I - p_h \right|\!\right\|_{Q_h} \leq Ch \left(\|\boldsymbol{F} - R(\boldsymbol{F}_h)\|_{H(div,\Omega)} + \|p\|_{H^1(\Omega)} + \|p - p_h\|_{L^2(\Omega)} \right). \tag{3.9}$$

Moreover, for piecewise constant diffusion tensors and convection fields in V_h, *it holds*

$$\left\|\!\left| p^I - p_h \right|\!\right\|_{Q_h} \leq Ch \left(\|\boldsymbol{F} - R(\boldsymbol{F}_h)\|_{H(div,\Omega)} + h\|p\|_{H^1(\Omega)} + \|p - p_h\|_{L^2(\Omega)} \right). \tag{3.10}$$

Proof. We recall that mimetic scalar fields are identified with piecewise constant functions so that

$$\left|\!\left|\!\left| p^I - p_h \right|\!\right|\!\right|_{Q_h} = \left\| p^I - p_h \right\|_{L^2(\Omega)}, \tag{3.11}$$

and we can proceed by bounding this latter quantity. For this purpose, we consider the dual problem:

$$-\mathrm{div}(K\nabla\varphi) + \boldsymbol{b}\cdot\nabla\varphi + c\varphi = p^I - p_h \qquad \text{in } \Omega, \tag{3.12a}$$

$$\varphi = 0 \qquad \text{on } \partial\Omega. \tag{3.12b}$$

As we assume that Ω is a convex domain with Lipschitz boundary, the solution φ belongs to $H^2(\Omega)$ and the stability inequality

$$\|\varphi\|_{H^2(\Omega)} \leq C \left\| p^I - p_h \right\|_{L^2(\Omega)} \tag{3.13}$$

holds. Using the orthogonality relation (3.4a) with $\boldsymbol{v} = K\nabla\varphi$ and $w = p^I - p_h$, and (3.4b) with $\boldsymbol{v} = R(K\nabla\varphi)^I$ and $w = p$, we have

$$\begin{aligned} \left\| p^I - p_h \right\|^2_{L^2(\Omega)} &= \left(p^I - p_h, -\mathrm{div}(K\nabla\varphi) + \boldsymbol{b}\cdot\nabla\varphi + c\varphi\right) \\ &= -\left(p^I - p_h, \mathrm{div}R(K\nabla\varphi)^I\right) + \left(p^I - p_h, \boldsymbol{b}\cdot\nabla\varphi + c\varphi\right) \\ &= -\left(p - p_h, \mathrm{div}R(K\nabla\varphi)^I\right) + \left(p^I - p_h, \boldsymbol{b}\cdot\nabla\varphi + c\varphi\right). \end{aligned} \tag{3.14}$$

From the first error equation (3.1a) with $\boldsymbol{v} = R(K\nabla\varphi)^I$, we obtain

$$\begin{aligned} \left(p - p_h, \mathrm{div}R(K\nabla\varphi)^I\right) &= \left(\alpha(\boldsymbol{F} - R(\boldsymbol{F}_h)), R(K\nabla\varphi)^I\right) \\ &\quad + \left(\alpha\left(\boldsymbol{b}p - R\left(\boldsymbol{b}^I\right)p_h\right), R(K\nabla\varphi)^I\right) \\ &\quad + \left((\alpha - \widetilde{\alpha})\left(R(\boldsymbol{F}_h) + R\left(\boldsymbol{b}^I\right)p_h\right), R(K\nabla\varphi)^I\right). \end{aligned} \tag{3.15}$$

The first term of the right-hand side of (3.15) can be further manipulated by adding and subtracting $K\nabla\varphi$

$$\begin{aligned} \left(\alpha(\boldsymbol{F} - R(\boldsymbol{F}_h)), R(K\nabla\varphi)^I\right) &= (\boldsymbol{F} - R(\boldsymbol{F}_h), \nabla\varphi) \\ &\quad + \left(\alpha(\boldsymbol{F} - R(\boldsymbol{F}_h)), R(K\nabla\varphi)^I - K\nabla\varphi\right) \end{aligned} \tag{3.16}$$

as $\alpha K = \mathbb{I}$. Since $\varphi = 0$ on the domain boundary, the Green formula and the second error equation (3.1b) with $w = \varphi^I$ allow us to further develop the first scalar product in the right-hand side of the last equality of (3.16) as

$$\begin{aligned} (\boldsymbol{F} - R(\boldsymbol{F}_h), \nabla\varphi) &= -\left(\mathrm{div}(\boldsymbol{F} - R(\boldsymbol{F}_h)), \varphi\right) \\ &= -\left(\mathrm{div}(\boldsymbol{F} - R(\boldsymbol{F}_h)) + cp - c^I p_h, \varphi\right) + \left(cp - c^I p_h, \varphi\right) \\ &= -\left(\mathrm{div}(\boldsymbol{F} - R(\boldsymbol{F}_h)) + cp - c^I p_h, \varphi - \varphi^I\right) + \left(cp - c^I p_h, \varphi\right). \end{aligned}$$

Further, we note that the second term of the right-hand side of (3.14) can be written as

$$\left(p^I - p_h, \boldsymbol{b}\cdot\nabla\varphi + c\varphi\right) = \left(\alpha\left(p^I - p_h\right)\boldsymbol{b}, K\nabla\varphi\right) + \left(c\left(p^I - p_h\right), \varphi\right). \tag{3.17}$$

Substituting the developments from (3.15)–(3.17) into (3.14) yields the final form

$$\left\|p^I - p_h\right\|^2_{L^2(\Omega)} = \mathsf{A} + \mathsf{B} + \mathsf{C} + \mathsf{D}, \tag{3.18}$$

where

$$\begin{aligned}
\mathsf{A} &= -\left(\alpha(\boldsymbol{F} - R(\boldsymbol{F}_h)), R(K\nabla\varphi)^I - K\nabla\varphi\right) + \left(\operatorname{div}(\boldsymbol{F} - R(\boldsymbol{F}_h)), \varphi - \varphi^I\right),\\
\mathsf{B} &= -\left(\alpha\left(\boldsymbol{b}p - R\left(\boldsymbol{b}^I\right)p_h\right), R(K\nabla\varphi)^I\right) + \left(\alpha\boldsymbol{b}\left(p^I - p_h\right), K\nabla\varphi\right),\\
\mathsf{C} &= \left(c\left(p^I - p_h\right), \varphi\right) + \left(cp - c^I p_h, \varphi - \varphi^I\right) - \left(cp - c^I p_h, \varphi\right),\\
\mathsf{D} &= \left((\alpha - \widetilde{\alpha})\left(R(\boldsymbol{F}_h) + R\left(\boldsymbol{b}^I\right)p_h\right), R(K\nabla\varphi)^I\right).
\end{aligned}$$

Before embarking on the estimate of these terms, we note that the following inequalities hold true:

$$\left\|R(K\nabla\varphi)^I - K\nabla\varphi\right\|_{L^2(\Omega)} \le Ch\|\varphi\|_{H^2(\Omega)}, \tag{3.19a}$$

$$\left\|R(K\nabla\varphi)^I\right\|_{L^2(\Omega)} \le C\left(\|\varphi\|_{H^1(\Omega)} + h\|\varphi\|_{H^2(\Omega)}\right). \tag{3.19b}$$

Indeed,

$$\begin{aligned}
\left\|R(K\nabla\varphi)^I - K\nabla\varphi\right\|^2_{L^2(\Omega)} &= \sum_{E\in\mathcal{T}_h}\left\|R(K\nabla\varphi)^I - K\nabla\varphi\right\|^2_{L^2(E)} \text{(by Lemma 3.2)}\\
&\le \sum_{E\in\mathcal{T}_h} Ch_E^2\|K\nabla\varphi\|^2_{H^1(E)}\\
&\le Ch^2\sum_{E\in\mathcal{T}_h}\|K\|^2_{W^{1,\infty}(E)}\|\varphi\|^2_{H^2(E)} \text{(by (K))}\\
&\le Ch^2\sum_{E\in\mathcal{T}_h}\|\varphi\|^2_{H^2(E)}
\end{aligned}$$

and

$$\begin{aligned}
\left\|R(K\nabla\varphi)^I\right\|_{L^2(\Omega)} &\le \|K\nabla\varphi\|_{L^2(\Omega)} + \left\|R(K\nabla\varphi)^I - K\nabla\varphi\right\|_{L^2(\Omega)}\\
&\le \|K\|_{L^\infty(\Omega)}\|\varphi\|_{H^1(\Omega)} + Ch\|\varphi\|_{H^2(\Omega)}\\
&\le C\left(\|\varphi\|_{H^1(\Omega)} + h\|\varphi\|_{H^2(\Omega)}\right),
\end{aligned}$$

where the final constant C absorbs the norm of K and is independent of h.

Bound of term A.

By the Cauchy–Schwarz inequality,

$$\begin{aligned}
|\mathsf{A}| \le{}& \|\alpha(\boldsymbol{F} - R(\boldsymbol{F}_h))\|_{L^2(\Omega)}\left\|R(K\nabla\varphi)^I - K\nabla\varphi\right\|_{L^2(\Omega)}\\
&+ \|\operatorname{div}(\boldsymbol{F} - R(\boldsymbol{F}_h))\|_{L^2(\Omega)}\left\|\varphi - \varphi^I\right\|_{L^2(\Omega)}.
\end{aligned}$$

Therefore, by using (3.19) and a standard interpolation error estimate, we obtain

$$\begin{aligned}
|\mathsf{A}| &\le Ch\|\alpha\|_{L^\infty(\Omega)}\|\boldsymbol{F} - R(\boldsymbol{F}_h)\|_{L^2(\Omega)}\ \|\varphi\|_{H^2(\Omega)}\\
&\quad + \|\operatorname{div}(\boldsymbol{F} - R(\boldsymbol{F}_h))\|_{L^2(\Omega)}\ \left\|\varphi - \varphi^I\right\|_{L^2(\Omega)}\\
&\le Ch\left(\|\boldsymbol{F} - R(\boldsymbol{F}_h)\|_{L^2(\Omega)} + \|\operatorname{div}(\boldsymbol{F} - R(\boldsymbol{F}_h))\|_{L^2(\Omega)}\right)\|\varphi\|_{H^2(\Omega)}.
\end{aligned} \tag{3.20}$$

Bound of term B.
By adding and subtracting $R(\boldsymbol{b}^I)p^I$ and $K\nabla\varphi$ we get

$$\begin{aligned}
\mathsf{B} &= -\left(\alpha\left(\boldsymbol{b}p - R\left(\boldsymbol{b}^I\right)p^I + R\left(\boldsymbol{b}^I\right)\left(p^I - p_h\right)\right), R(K\nabla\varphi)^I\right) + \left(\alpha\boldsymbol{b}\left(p^I - p_h\right), K\nabla\varphi\right)\\
&= -\left(\alpha\left(\boldsymbol{b}p - R\left(\boldsymbol{b}^I\right)p^I\right), R(K\nabla\varphi)^I\right) - \left(\alpha R\left(\boldsymbol{b}^I\right)\left(p^I - p_h\right), K\nabla\varphi\right)\\
&\quad -\left(\alpha R\left(\boldsymbol{b}^I\right)\left(p^I - p_h\right), R(K\nabla\varphi)^I - K\nabla\varphi\right) + \left(\alpha\boldsymbol{b}\left(p^I - p_h\right), K\nabla\varphi\right)\\
&= -\left(\alpha\left(\boldsymbol{b}p - R\left(\boldsymbol{b}^I\right)p^I\right), R(K\nabla\varphi)^I\right) - \left(\alpha R\left(\boldsymbol{b}^I\right)\left(p^I - p_h\right), R(K\nabla\varphi)^I - K\nabla\varphi\right)\\
&\quad + \left(\alpha\left(\boldsymbol{b} - R\left(\boldsymbol{b}^I\right)\right)\left(p^I - p_h\right), K\nabla\varphi\right) = \mathsf{B}_1 + \mathsf{B}_2 + \mathsf{B}_3.
\end{aligned}$$

As far as B_1 is concerned, the Cauchy–Schwarz inequality yields

$$|\mathsf{B}_1| \le \left\|\alpha\left(\boldsymbol{b}p - R\left(\boldsymbol{b}^I\right)p^I\right)\right\|_{L^2(\Omega)} \left\|R(K\nabla\varphi)^I\right\|_{L^2(\Omega)}.$$

Further, note that

$$\begin{aligned}
\left\|\alpha\left(\boldsymbol{b}p - R\left(\boldsymbol{b}^I\right)p^I\right)\right\|_{L^2(\Omega)} &\le C_\alpha\left\|\left(\boldsymbol{b} - R\left(\boldsymbol{b}^I\right)\right)p\right\|_{L^2(\Omega)} + C_\alpha\left\|R\left(\boldsymbol{b}^I\right)\left(p - p^I\right)\right\|_{L^2(\Omega)}\\
&\le Ch\|\boldsymbol{b}\|_{W^{1,\infty}(\Omega)}\|p\|_{L^2(\Omega)} + Ch\|\boldsymbol{b}\|_{L^\infty(\Omega)}\|p\|_{H^1(\Omega)}.
\end{aligned}$$

Thus, using (3.19b),

$$|\mathsf{B}_1| \le Ch(1+Ch)\|\boldsymbol{b}\|_{W^{1,\infty}(\Omega)}\|p\|_{H^1(\Omega)}\|\varphi\|_{H^2(\Omega)}. \tag{3.21}$$

Let us consider here the special case $\boldsymbol{b} \in V_h$, which implies that $\boldsymbol{b} = R(\boldsymbol{b}^I)$. The terms related to this particular case are marked by an asterisk to distinguish them from those referring to the more general case, e.g., B^* and B_1^* instead of B and B_1. We rearrange the term B_1^* as follows:

$$\begin{aligned}
\mathsf{B}_1^* &= -\left(\boldsymbol{b}p - R\left(\boldsymbol{b}^I\right)p^I, \nabla\varphi\right) - \left(\alpha\left(\boldsymbol{b}p - R\left(\boldsymbol{b}^I\right)p^I\right), R(K\nabla\varphi)^I - K\nabla\varphi\right)\\
&= -\left(\boldsymbol{b}\left(p - p^I\right), \nabla\varphi\right) - \left(\alpha\boldsymbol{b}\left(p - p^I\right), R(K\nabla\varphi)^I - K\nabla\varphi\right)\\
&= \mathsf{B}_{1,1}^* + \mathsf{B}_{1,2}^*.
\end{aligned}$$

Note that

$$\mathsf{B}_{1,1}^* = \left(p - p^I, \boldsymbol{b}\cdot\nabla\varphi\right) = \left(p - p^I, \boldsymbol{b}\cdot\nabla\varphi - (\boldsymbol{b}\cdot\nabla\varphi)^I\right),$$

and thus

$$\begin{aligned}
|\mathsf{B}_{1,1}^*| &\le Ch^2\|p\|_{H^1(\Omega)}\|\boldsymbol{b}\cdot\nabla\varphi\|_{H^1(\Omega)}\\
&\le Ch^2\|\boldsymbol{b}\|_{W^{1,\infty}(\Omega)}\|p\|_{H^1(\Omega)}\|\varphi\|_{H^2(\Omega)}.
\end{aligned}$$

On its turn, by (3.19a)

$$\mathsf{B}_{1,2}^* \le Ch^2\|\boldsymbol{b}\|_{L^\infty(\Omega)}\|p\|_{H^1(\Omega)}\|\varphi\|_{H^2(\Omega)}.$$

Thus,

$$|\mathsf{B}_1^*| \le Ch^2\|\boldsymbol{b}\|_{W^{1,\infty}(\Omega)}\|p\|_{H^1(\Omega)}\|\varphi\|_{H^2(\Omega)}. \tag{3.22}$$

The term B_2 is controlled by using the Cauchy–Schwarz inequality and Lemma 3.2 with $\boldsymbol{v} = K\nabla\varphi$:

$$\begin{aligned} |\mathsf{B}_2| &\le \left\| \alpha R\left(\boldsymbol{b}^I\right)\left(p^I - p_h\right)\right\|_{L^2(\Omega)} \left\| R(K\nabla\varphi)^I - K\nabla\varphi\right\|_{L^2(\Omega)} \\ &\le Ch\|\boldsymbol{b}\|_{L^\infty(\Omega)} \left\|p^I - p_h\right\|_{L^2(\Omega)} \|\varphi\|_{H^2(\Omega)}. \end{aligned} \tag{3.23}$$

Finally, the term B_3 is controlled by using the Cauchy–Schwarz inequality and Lemma 3.3:

$$\begin{aligned} |\mathsf{B}_3| &\le \left\| \left(\boldsymbol{b} - R\left(\boldsymbol{b}^I\right)\right)\left(p^I - p_h\right)\right\|_{L^2(\Omega)} \|\nabla\varphi\|_{L^2(\Omega)} \\ &\le Ch\|\boldsymbol{b}\|_{W^{1,\infty}(\Omega)} \left\|p^I - p_h\right\|_{L^2(\Omega)} \|\varphi\|_{H^1(\Omega)}. \end{aligned} \tag{3.24}$$

Collecting the estimates (3.21), (3.23), and (3.24) and absorbing the various norms of $\boldsymbol{b}$ in the symbol C yields

$$\begin{aligned} |\mathsf{B}| &\le |\mathsf{B}_1| + |\mathsf{B}_2| + |\mathsf{B}_3| \\ &\le Ch\left((1+Ch)\|p\|_{H^1(\Omega)} + \left\|p^I - p_h\right\|_{L^2(\Omega)}\right)\|\varphi\|_{H^2(\Omega)}, \end{aligned} \tag{3.25}$$

while, using (3.22) instead of (3.21), we obtain

$$|\mathsf{B}^*| \le |\mathsf{B}_1^*| + |\mathsf{B}_2| \le Ch\left(h\|p\|_{H^1(\Omega)} + \left\|p^I - p_h\right\|_{L^2(\Omega)}\right)\|\varphi\|_{H^2(\Omega)} \tag{3.26}$$

as B_3 is zero in this case.

Bound of term C.

Rearranging the first and last scalar products in C, we get

$$\mathsf{C} = \left(c\left(p^I - p\right), \varphi\right) + \left(cp - c^I p_h, \varphi - \varphi^I\right) + \left(\left(c^I - c\right)p_h, \varphi\right) = \mathsf{C}_1 + \mathsf{C}_2 + \mathsf{C}_3.$$

Adding and subtracting c^I and noting that $c^I\varphi^I$ is orthogonal to $p^I - p$ allows us to transform C_1 as follows:

$$\begin{aligned} \mathsf{C}_1 &= \left(\left(c - c^I\right)\left(p^I - p\right), \varphi\right) + \left(c^I\left(p^I - p\right), \varphi\right) \\ &= \left(\left(c - c^I\right)\left(p^I - p\right), \varphi\right) + \left(c^I\left(p^I - p\right), \varphi - \varphi^I\right). \end{aligned} \tag{3.27}$$

We estimate C_1 by applying the Cauchy–Schwarz inequality to both terms in the right-hand side of (3.27), using appropriate interpolation error bounds to $c - c^I$, $p^I - p$, and $\varphi - \varphi^I$, and finally by noting that $\|c^I\|_{L^\infty(\Omega)} \le \|c\|_{L^\infty(\Omega)}$:

$$\begin{aligned} |\mathsf{C}_1| &\le \left\|c - c^I\right\|_{L^\infty(\Omega)} \left\|p^I - p\right\|_{L^2(\Omega)} \|\varphi\|_{L^2(\Omega)} \\ &\quad + \left\|c^I\right\|_{L^\infty(\Omega)} \left\|p^I - p\right\|_{L^2(\Omega)} \left\|\varphi - \varphi^I\right\|_{L^2(\Omega)} \\ &\le Ch^2\left(\|c\|_{W^{1,\infty}(\Omega)}\|p\|_{H^1(\Omega)}\|\varphi\|_{L^2(\Omega)} + \|c\|_{L^\infty(\Omega)}\|p\|_{H^1(\Omega)}\|\varphi\|_{H^1(\Omega)}\right). \end{aligned} \tag{3.28}$$

To estimate C_2, we first note that adding/subtracting $c^I p$, using the triangle inequality, Lemma 3.4, and the fact that $\|c^I\|_{L^\infty(\Omega)} \le \|c\|_{L^\infty(\Omega)}$, gives

$$\begin{aligned} \left\|cp - c^I p_h\right\|_{L^2(\Omega)} &= \left\|\left(c - c^I\right)p - c^I(p_h - p)\right\|_{L^2(\Omega)} \\ &\le \left\|c - c^I\right\|_{L^\infty(\Omega)} \|p\|_{L^2(\Omega)} + \left\|c^I\right\|_{L^\infty(\Omega)} \|p_h - p\|_{L^2(\Omega)} \\ &\le Ch\|c\|_{W^{1,\infty}(\Omega)}\|p\|_{L^2(\Omega)} + \|c\|_{L^\infty(\Omega)}\|p_h - p\|_{L^2(\Omega)}. \end{aligned} \tag{3.29}$$

Thus, applying the Cauchy–Schwarz inequality and the L^2 error interpolation bound to $\varphi - \varphi^I$ yields

$$|\mathsf{C}_2| \leq C \left(h^2 \|c\|_{W^{1,\infty}(\Omega)} \|p\|_{L^2(\Omega)} + h\|c\|_{L^\infty(\Omega)} \|p_h - p\|_{L^2(\Omega)}\right) \|\varphi\|_{H^1(\Omega)}. \tag{3.30}$$

Note that

$$\left((c^I - c)\, p_h, \varphi^I\right) = \sum_{E\in\mathcal{T}_h} p_E \varphi^I|_E \int_E \left(c^I - c\right)\, dV = 0.$$

Thus, subtracting φ^I from φ in C_3, using once again the Cauchy–Schwarz inequality, adding and subtracting p, and exploiting the result of Lemma 3.4 and the L^2 error interpolation estimate for $\varphi - \varphi^I$ yields

$$\begin{aligned} |\mathsf{C}_3| &\leq \left\|c^I - c\right\|_{L^\infty(\Omega)} \left(\|p\|_{L^2(\Omega)} + \|p - p_h\|_{L^2(\Omega)}\right) \left\|\varphi - \varphi^I\right\|_{L^2(\Omega)} \\ &\leq Ch^2 \|c\|_{W^{1,\infty}(\Omega)} \left(\|p\|_{L^2(\Omega)} + \|p - p_h\|_{L^2(\Omega)}\right) \|\varphi\|_{H^1(\Omega)}. \end{aligned} \tag{3.31}$$

Collecting the estimates for the various terms composing C, i.e., (3.28), (3.30), and (3.31), yields the final estimate for this term:

$$\begin{aligned} |\mathsf{C}| \leq |\mathsf{C}_1| + |\mathsf{C}_2| + |\mathsf{C}_3| &\leq Ch\big(\|c\|_{W^{1,\infty}(\Omega)} \|p\|_{L^2(\Omega)} + \|c\|_{L^\infty(\Omega)} \|p\|_{H^1(\Omega)} \\ &\quad + \|c\|_{L^\infty(\Omega)} \|p_h - p\|_{L^2(\Omega)}\big) \|\varphi\|_{H^1(\Omega)} \\ &\leq Ch \left(h\|p\|_{H^1(\Omega)} + \|p_h - p\|_{L^2(\Omega)}\right) \|\varphi\|_{H^1(\Omega)}, \end{aligned} \tag{3.32}$$

where the constant C in the last inequality is absorbing the various norms of the scalar reaction field c.

Bound of term D.

First, note that this term is null when the diffusion tensor is piecewise constant on the mesh partition of Ω, i.e., $\widetilde{\alpha}_E = \alpha_E$ for every $E \in \mathcal{T}_h$. Otherwise, the term D can be rearranged as follows:

$$\begin{aligned} \mathsf{D} &= -\left((\alpha - \widetilde{\alpha})(\boldsymbol{F} - R(\boldsymbol{F}_h)), R(K\nabla\varphi)^I\right) - \left((\alpha - \widetilde{\alpha})\boldsymbol{b}(p - p_h), R(K\nabla\varphi)^I\right) \\ &\quad - \left((\alpha - \widetilde{\alpha}) \left(\boldsymbol{b} - R\left(\boldsymbol{b}^I\right)\right) p_h, R(K\nabla\varphi)^I\right) + \left((\alpha - \widetilde{\alpha})(\boldsymbol{F} + \boldsymbol{b}p), R(K\nabla\varphi)^I\right) \\ &= \mathsf{D}_1 + \mathsf{D}_2 + \mathsf{D}_3 + \mathsf{D}_4. \end{aligned}$$

By applying the Cauchy–Schwarz inequality, the bound (2.3) from assumption (K), and inequality (3.19b) and absorbing $\widetilde{C}_\alpha$ in the constant C independent of h, we obtain

$$|\mathsf{D}_1| \leq Ch\|\boldsymbol{F} - R(\boldsymbol{F}_h)\|_{L^2(\Omega)} \left(\|\varphi\|_{H^1(\Omega)} + h\|\varphi\|_{H^2(\Omega)}\right), \tag{3.33a}$$

$$|\mathsf{D}_2| \leq Ch\|\boldsymbol{b}\|_{L^\infty(\Omega)} \|p - p_h\|_{L^2(\Omega)} \left(\|\varphi\|_{H^1(\Omega)} + h\|\varphi\|_{H^2(\Omega)}\right), \tag{3.33b}$$

$$|\mathsf{D}_3| \leq Ch^2\|\boldsymbol{b}\|_{W^{1,\infty}(\Omega)} \left(\|p\|_{L^2(\Omega)} + \|p - p_h\|_{L^2(\Omega)}\right) \left(\|\varphi\|_{H^1(\Omega)} + h\|\varphi\|_{H^2(\Omega)}\right), \tag{3.33c}$$

$$|\mathsf{D}_4| \leq Ch\|K\nabla p\|_{L^2(\Omega)} \left(\|\varphi\|_{H^1(\Omega)} + h\|\varphi\|_{H^2(\Omega)}\right). \tag{3.33d}$$

By collecting the estimates (3.33a)–(3.33d) and absorbing in the symbol C all the norms of $\boldsymbol{b}$ we obtain the inequality

$$\begin{aligned} |\mathsf{D}| \leq Ch\big(&\|\boldsymbol{F} - R(\boldsymbol{F}_h)\|_{L^2(\Omega)} + (1 + Ch)\|p - p_h\|_{L^2(\Omega)} + h\|p\|_{L^2(\Omega)} \\ &+ \|p\|_{H^1(\Omega)}\big) \left(\|\varphi\|_{H^1(\Omega)} + h\|\varphi\|_{H^2(\Omega)}\right). \end{aligned} \tag{3.34}$$

Finally, replacing the estimates of terms A, B, C, and D, given by (3.20), (3.25), (3.32), and (3.34), respectively, into (3.18) and moving the terms containing $\|p^I - p_h\|_{L^2(\Omega)}$ to the left-hand side yields

$$(1 - Ch)\left\|p^I - p_h\right\|^2_{L^2(\Omega)} \leq Ch\big(\|\boldsymbol{F} - R(\boldsymbol{F}_h)\|_{H(\mathsf{div},\Omega)} + (1 + Ch)\|p\|_{H^1(\Omega)} + (1 + Ch)\|p - p_h\|_{L^2(\Omega)}\big)\|\varphi\|_{H^2(\Omega)},$$

from which (3.9) readily follows due to (3.13). Likewise, inequality (3.10) follows by using the estimate (3.26) for the term B^* instead of the more general estimate (3.25) and noting that $\mathsf{D} = 0$ in the case of piecewise constant diffusion tensors (e.g., $\alpha = \widetilde{\alpha}$). ∎

The mesh-dependent error $\|\boldsymbol{F}^I - \boldsymbol{F}_h\|_{X_h}$ is estimated as follows.

LEMMA 3.7. *Under assumptions* (H)–(K), (L1)–(L2), (M1)–(M5), *and* (S1)–(S2), *it holds*

$$\left|\!\left|\!\left|\boldsymbol{F}^I - \boldsymbol{F}_h\right|\!\right|\!\right|_{X_h} \leq C\left(h\|p\|_{H^2(\Omega)} + \|p - p_h\|_{L^2(\Omega)}\right), \tag{3.35}$$

where $C = C(\|\boldsymbol{b}\|_{W^{1,\infty}(\Omega)}, \|c\|_{W^{1,\infty}(\Omega)})$ *is independent of* h.

Proof. Developing the definition of $|\!|\!|\cdot|\!|\!|_{X_h}$ and adding and subtracting terms we obtain

$$\begin{aligned}\left|\!\left|\!\left|\boldsymbol{F}^I - \boldsymbol{F}_h\right|\!\right|\!\right|^2_{X_h} &= \left(\alpha\boldsymbol{F} - \widetilde{\alpha}R(\boldsymbol{F}_h), R\left(\boldsymbol{F}^I - \boldsymbol{F}_h\right)\right)\\ &\quad + \left((\widetilde{\alpha} - \alpha)\boldsymbol{F}, R\left(\boldsymbol{F}^I - \boldsymbol{F}_h\right)\right)\\ &\quad + \left(\widetilde{\alpha}\left(R\left(\boldsymbol{F}^I\right) - \boldsymbol{F}\right), R\left(\boldsymbol{F}^I - \boldsymbol{F}_h\right)\right) = \mathsf{E}_1 + \mathsf{E}_2 + \mathsf{E}_3.\end{aligned}$$

Substituting the first error equation (3.1a) applied with $\boldsymbol{v} = R(\boldsymbol{F}^I - \boldsymbol{F}_h)$ and using (3.7), the term E_1 is further developed as follows:

$$\begin{aligned}\mathsf{E}_1 &= \left(p - p_h, \mathrm{div}R\left(\boldsymbol{F}^I - \boldsymbol{F}_h\right)\right) - \left(\alpha\boldsymbol{b}p - \widetilde{\alpha}R\left(\boldsymbol{b}^I\right)p_h, R\left(\boldsymbol{F}^I - \boldsymbol{F}_h\right)\right)\\ &= \left(p - p_h, c^I p_h - (cp)^I\right) - \left(\widetilde{\alpha}\left(\boldsymbol{b}p - R\left(\boldsymbol{b}^I\right)p_h\right), R\left(\boldsymbol{F}^I - \boldsymbol{F}_h\right)\right)\\ &\quad - \left((\alpha - \widetilde{\alpha})\boldsymbol{b}p, R\left(\boldsymbol{F}^I - \boldsymbol{F}_h\right)\right).\end{aligned}$$

Thus, applying the Cauchy–Schwarz inequality gives

$$\begin{aligned}|\mathsf{E}_1| &\leq \|p - p_h\|_{L^2(\Omega)}\left\|c^I p_h - (cp)^I\right\|_{L^2(\Omega)}\\ &\quad + \left\|\widetilde{\alpha}^{1/2}\left(\boldsymbol{b}p - R\left(\boldsymbol{b}^I\right)p_h\right)\right\|_{L^2(\Omega)}\left\|\widetilde{\alpha}^{1/2}R\left(\boldsymbol{F}^I - \boldsymbol{F}_h\right)\right\|_{L^2(\Omega)}\\ &\quad + \left\|\widetilde{\alpha}^{-1/2}(\alpha - \widetilde{\alpha})\boldsymbol{b}p\right\|_{L^2(\Omega)}\left\|\widetilde{\alpha}^{1/2}R\left(\boldsymbol{F}^I - \boldsymbol{F}_h\right)\right\|_{L^2(\Omega)}.\end{aligned}$$

To work out the term $\|c^I p_h - cp\|_{L^2(\Omega)}$ we add and subtract cp, and apply the triangular inequality. In this way, we get the term already controlled in (3.29) and a term containing an interpolation error for cp:

$$\begin{aligned}\left\|c^I p_h - (cp)^I\right\|_{L^2(\Omega)} &\leq \left\|c^I p_h - cp\right\|_{L^2(\Omega)} + \left\|cp - (cp)^I\right\|_{L^2(\Omega)}\\ &\leq C\left(h\|c\|_{W^{1,\infty}(\Omega)}\|p\|_{L^2(\Omega)} + \|c\|_{L^\infty(\Omega)}\|p_h - p\|_{L^2(\Omega)}\right).\end{aligned}$$

The second term bounding $|\mathsf{E}_1|$ is controlled by noting that

$$\begin{aligned}
&\left\|\widetilde{\alpha}^{1/2}\left(\boldsymbol{b}p - R\left(\boldsymbol{b}^I\right)p_h\right)\right\|^2_{L^2(\Omega)} \\
&\quad\le \sum_{E\in\mathcal{T}_h}\left\|\alpha^{1/2}\left(\boldsymbol{b}p - R\left(\boldsymbol{b}^I\right)p_h\right)\right\|^2_{L^2(E)} \\
&\qquad+ \sum_{E\in\mathcal{T}_h}\left\|\left(\widetilde{\alpha}^{1/2}-\alpha^{1/2}\right)\left(\boldsymbol{b}p - R\left(\boldsymbol{b}^I\right)p_h\right)\right\|^2_{L^2(E)} \\
&\quad\le C_\alpha\sum_{E\in\mathcal{T}_h}\left\|\boldsymbol{b}p - R\left(\boldsymbol{b}^I\right)p_h\right\|^2_{L^2(E)} + \widetilde{C}_\alpha\sum_{E\in\mathcal{T}_h}h_E\left\|\boldsymbol{b}p - R\left(\boldsymbol{b}^I\right)p_h\right\|^2_{L^2(E)} \\
&\quad\le \left(C_\alpha + \widetilde{C}_\alpha h\right)\left\|\boldsymbol{b}p - R\left(\boldsymbol{b}^I\right)p_h\right\|^2_{L^2(\Omega)},
\end{aligned}$$

and thus,

$$\begin{aligned}
&\left\|\widetilde{\alpha}^{1/2}\left(\boldsymbol{b}p - R\left(\boldsymbol{b}^I\right)p_h\right)\right\|_{L^2(\Omega)} \\
&\quad\le C\left(\left\|\left(\boldsymbol{b} - R\left(\boldsymbol{b}^I\right)\right)p\right\|_{L^2(\Omega)} + \left\|R\left(\boldsymbol{b}^I\right)(p-p_h)\right\|_{L^2(\Omega)}\right) \\
&\quad\le C\left(h\|\boldsymbol{b}\|_{W^{1,\infty}(\Omega)}\|p\|_{L^2(\Omega)} + \|\boldsymbol{b}\|_{L^\infty(\Omega)}\|p-p_h\|_{L^2(\Omega)}\right),
\end{aligned} \tag{3.36}$$

which follows from the Cauchy–Schwarz inequality, the boundedness of the lifting operator R (arguing as in (3.19b)), assumptions (K), and the interpolation error bound (3.5) of Lemma 3.3. By noting that $\|\boldsymbol{F}^I - \boldsymbol{F}_h\|_{X_h} = \|\widetilde{\alpha}^{1/2}R(\boldsymbol{F}^I - \boldsymbol{F}_h)\|_{L^2(\Omega)}$ and absorbing the various norms of $\boldsymbol{b}$ and c in C, we obtain

$$\begin{aligned}
|\mathsf{E}_1| &\le C\left(h\|p\|_{L^2(\Omega)} + \|p_h - p\|_{L^2(\Omega)}\right)\|p-p_h\|_{L^2(\Omega)} \\
&\quad + C\left(h\|p\|_{L^2(\Omega)} + \|p-p_h\|_{L^2(\Omega)}\right)\left|\!\left|\!\left|\boldsymbol{F}^I - \boldsymbol{F}_h\right|\!\right|\!\right|_{X_h} \\
&\le \left(h\|p\|_{L^2(\Omega)} + \|p_h - p\|_{L^2(\Omega)}\right)\|p-p_h\|_{L^2(\Omega)} \\
&\quad + \frac{C^2}{2}\left(h\|p\|_{L^2(\Omega)} + \|p-p_h\|_{L^2(\Omega)}\right)^2 + \frac{1}{2}\left|\!\left|\!\left|\boldsymbol{F}^I - \boldsymbol{F}_h\right|\!\right|\!\right|^2_{X_h}.
\end{aligned}$$

The term E_2 is bounded as the last term of E_1:

$$\begin{aligned}
|\mathsf{E}_2| &= \left|\left(\widetilde{\alpha}^{-1/2}(\widetilde{\alpha}-\alpha)R\left(\boldsymbol{F}^I - \boldsymbol{F}_h\right), \widetilde{\alpha}^{1/2}R\left(\boldsymbol{F}^I - \boldsymbol{F}_h\right)\right)\right| \\
&\le Ch\left\|\widetilde{\alpha}^{1/2}R\left(\boldsymbol{F}^I - \boldsymbol{F}_h\right)\right\|^2_{L^2(\Omega)} \\
&= Ch\left|\!\left|\!\left|\boldsymbol{F}^I - \boldsymbol{F}_h\right|\!\right|\!\right|^2_{X_h},
\end{aligned}$$

where C is independent of h and absorbs the constant factors depending on the regularity of α. Finally,

$$\begin{aligned}
|\mathsf{E}_3| &\le C\left\|\widetilde{\alpha}^{1/2}\left(R\left(\boldsymbol{F}^I\right) - \boldsymbol{F}\right)\right\|_{L^2(\Omega)}\left\|\widetilde{\alpha}^{1/2}R\left(\boldsymbol{F}^I - \boldsymbol{F}_h\right)\right\|_{L^2(\Omega)} \\
&= Ch\|p\|_{H^2(\Omega)}\left|\!\left|\!\left|\boldsymbol{F}^I - \boldsymbol{F}_h\right|\!\right|\!\right|_{X_h} \\
&\le C\frac{h}{2}\left(\|p\|^2_{H^2(\Omega)} + \left|\!\left|\!\left|\boldsymbol{F}^I - \boldsymbol{F}_h\right|\!\right|\!\right|^2_{X_h}\right).
\end{aligned}$$

By combining the estimates for E_1, E_2, and E_3 we obtain

$$(1 - Ch) \left|\!\left|\!\left| \boldsymbol{F}^I - \boldsymbol{F}_h \right|\!\right|\!\right|_{X_h}^2 \leq C \left(h\|p\|_{H^2(\Omega)} + \|p - p_h\|_{L^2(\Omega)} \right)^2,$$

and inequality (3.35) follows for h small enough. ∎

We end this subsection by the following technical lemma.

LEMMA 3.8. *Under assumptions* (H)–(K), (L1)–(L2), (M1)–(M5), and (S1)–(S2) *and for small enough h it holds*

$$\|\boldsymbol{F} - R(\boldsymbol{F}_h)\|_{H(\mathsf{div},\Omega)} \leq C \left(h\|p\|_{H^2(\Omega)} + \|p - p_h\|_{L^2(\Omega)} + \left\|f - f^I\right\|_{L^2(\Omega)} \right). \tag{3.37}$$

Proof. The L^2 term is controlled by adding and subtracting $R(\boldsymbol{F}^I)$, using Lemma 3.2, multiplying the argument of the second norm by $\widetilde{\alpha}^{-1/2}\widetilde{\alpha}^{1/2}$, arguing as in (3.36), and finally using Lemma 3.7:

$$\begin{aligned} \|\boldsymbol{F} - R(\boldsymbol{F}_h)\|_{L^2(\Omega)} &\leq \left\|\boldsymbol{F} - R\left(\boldsymbol{F}^I\right)\right\|_{L^2(\Omega)} + C \left\|\widetilde{\alpha}^{1/2} R\left(\boldsymbol{F}^I - \boldsymbol{F}_h\right)\right\|_{L^2(\Omega)} \\ &\leq C \left(h\|p\|_{H^2(\Omega)} + \left|\!\left|\!\left| \boldsymbol{F}^I - \boldsymbol{F}_h \right|\!\right|\!\right|_{X_h} \right) \\ &\leq C \left(h\|p\|_{H^2(\Omega)} + \|p - p_h\|_{L^2(\Omega)} \right). \end{aligned} \tag{3.38}$$

Similarly, to control the divergence error we employ (3.3) to get

$$\begin{aligned} \|\mathrm{div}(\boldsymbol{F} - R(\boldsymbol{F}_h))\|_{L^2(\Omega)} &\leq \left\|cp - c^I p_h\right\|_{L^2(\Omega)} + \left\|f - f^I\right\|_{L^2(\Omega)} \\ &\leq \left\|\left(c - c^I\right) p\right\|_{L^2(\Omega)} + \left\|c^I (p - p_h)\right\|_{L^2(\Omega)} + \left\|f - f^I\right\|_{L^2(\Omega)} \\ &\leq C \big(h\|p\|_{L^2(\Omega)} + \|p - p_h\|_{L^2(\Omega)} + \left\|f - f^I\right\|_{L^2(\Omega)} \big). \end{aligned} \tag{3.39}$$

Inequality (3.37) follows by combining estimates (3.38) and (3.39). ∎

3.3. A priori estimates. Our first two theorems state the error estimates in the $L^2(\Omega)$-norm for the scalar solution and in the $H(\mathsf{div},\Omega)$-norm for the flux field. Both estimates provide a convergence rate which is of order h.

THEOREM 3.9. *Let Ω be a convex domain with Lipschitz continuous boundary. Under assumptions* (H)–(K), (L1)–(L2), (M1)–(M5), and (S1)–(S2) *and for h small enough it holds*

$$\|p - p_h\|_{L^2(\Omega)} \leq Ch \left(\|p\|_{H^1(\Omega)} + h\|p\|_{H^2(\Omega)} + \left\|f - f^I\right\|_{L^2(\Omega)} \right). \tag{3.40}$$

Proof. Adding and subtracting p^I, using the triangular inequality, the standard estimate for the interpolation error $\|p - p^I\|_{L^2(\Omega)}$ and (3.11) yield

$$\begin{aligned} \|p - p_h\|_{L^2(\Omega)} &\leq \left\|p - p^I\right\|_{L^2(\Omega)} + \left\|p^I - p_h\right\|_{L^2(\Omega)} \\ &\leq Ch\|p\|_{H^1(\Omega)} + \left|\!\left|\!\left| p^I - p_h \right|\!\right|\!\right|_{Q_h}. \end{aligned} \tag{3.41}$$

The error $\left|\!\left|\!\left| p^I - p_h \right|\!\right|\!\right|_{Q_h}$ is estimated in Lemma 3.6 in terms of flux errors. Thus, using inequality (3.37) in (3.9) yields

$$\left|\!\left|\!\left| p^I - p_h \right|\!\right|\!\right|_{Q_h} \leq Ch \left(\|p\|_{H^1(\Omega)} + h\|p\|_{H^2(\Omega)} + \|p - p_h\|_{L^2(\Omega)} + \left\|f - f^I\right\|_{L^2(\Omega)} \right). \tag{3.42}$$

Substituting (3.42) into (3.41) and moving to the left-hand side the term containing $Ch\|p-p_h\|_{L^2(\Omega)}$ results in an inequality of the form

$$(1-Ch)\|p-p_h\|_{L^2(\Omega)} \leq Ch\left(\|p\|_{H^1(\Omega)} + h\|p\|_{H^2(\Omega)} + \left\|f-f^I\right\|_{L^2(\Omega)}\right),$$

from which inequality (3.40) follows for small enough h. ∎

THEOREM 3.10. *Let Ω be a convex domain with Lipschitz continuous boundary. Under assumptions* (H)–(K), (L1)–(L2), (M1)–(M5), and (S1)–(S2) *and for small enough h it holds*

$$\|\boldsymbol{F} - R(\boldsymbol{F}_h)\|_{H(\mathit{div},\Omega)} \leq Ch\|p\|_{H^2(\Omega)} + \left\|f-f^I\right\|_{L^2(\Omega)}. \tag{3.43}$$

Moreover, if $f \in H^1(\Omega)$, then

$$\|\boldsymbol{F} - R(\boldsymbol{F}_h)\|_{H(\mathit{div},\Omega)} \leq Ch\left(\|p\|_{H^2(\Omega)} + \|f\|_{H^1(\Omega)}\right). \tag{3.44}$$

Proof. We get the estimate (3.43) by substituting (3.40) into (3.37). Further, the bound (3.44) follows by applying a standard estimate for the interpolation error $\|f-f^I\|_{L^2(\Omega)}$ to (3.43). ∎

The errors in the mesh-dependent norms are estimated in the following two theorems.

THEOREM 3.11. *Let Ω be a convex domain with Lipschitz continuous boundary. Under assumptions* (H)–(K), (L1)–(L2), (M1)–(M5), and (S1)–(S2) *and for small enough h it holds*

$$\left|\!\left|\!\left|p^I - p_h\right|\!\right|\!\right|_{Q_h} \leq Ch\left(\|p\|_{H^1(\Omega)} + h\|p\|_{H^2(\Omega)} + \left\|f-f^I\right\|_{L^2(\Omega)}\right). \tag{3.45}$$

Moreover, assuming that the diffusion tensor is piecewise constant and the convection field belongs to V_h, we have

$$\left|\!\left|\!\left|p^I - p_h\right|\!\right|\!\right|_{Q_h} \leq Ch\left(h\|p\|_{H^2(\Omega)} + \left\|f-f^I\right\|_{L^2(\Omega)}\right). \tag{3.46}$$

If $f \in H^1(\Omega)$, we obtain the superconvergence result

$$\left|\!\left|\!\left|p^I - p_h\right|\!\right|\!\right|_{Q_h} \leq Ch^2\left(\|p\|_{H^2(\Omega)} + \|f\|_{H^1(\Omega)}\right). \tag{3.47}$$

Proof. Inequality (3.45) follows by using (3.37) in (3.9) (cf. the derivation of (3.42)) and employing (3.40) to bound the L^2-norm of (p^I-p_h). The extra assumptions on the diffusion tensor and the convection field imply that $\alpha = \widetilde{\alpha}$ and $\boldsymbol{b} = R(\boldsymbol{b}^I)$. Thus, we can use (3.10) instead of (3.9) to obtain (3.46). If $f \in H^1(\Omega)$, the term $\|f-f^I\|_{L^2(\Omega)}$ is further developed by applying a standard interpolation error estimate, thus giving the superconvergence result (3.47). ∎

THEOREM 3.12. *Let Ω be a convex domain with Lipschitz continuous boundary. Under assumptions* (H)–(K), (L1)–(L2), (M1)–(M5), and (S1)–(S2) *and for small enough h it holds*

$$\left|\!\left|\!\left|\boldsymbol{F}^I - \boldsymbol{F}_h\right|\!\right|\!\right|_{X_h} \leq Ch\left(\|p\|_{H^2(\Omega)} + \left\|f-f^I\right\|_{L^2(\Omega)}\right). \tag{3.48}$$

Proof. Inequality (3.48) is obtained by substituting (3.40) from Theorem 3.9 into (3.35) from Lemma 3.7. ∎

4. Numerical experiments. The numerical experiments presented in this section are aimed at confirming the a priori analysis. We solve problem (1.1) on the domain $\Omega =]0,1[\times]0,1[$ using the following data:

- *test* 1: the diffusion tensor K is given by the 2×2 identity matrix, the velocity field is given by $\boldsymbol{b}(x,y) = (1,3)^T$, and the reaction field is given by $c(x,y) = xy^2$;
- *test* 2: the diffusion tensor is given by

$$K(x,y) = \begin{pmatrix} (x+1)^2+y^2 & -xy \\ -xy & (x+1)^2 \end{pmatrix},$$

the velocity field is given by $\boldsymbol{b}(x,y) = xy(1-x)(1-y)(1,3)^T$, and the reaction field is given by $c(x,y) = xy^2$.

In both test cases, the forcing term f and the boundary condition g are set in accordance with

$$p(x,y) = \sin(2\pi x)\sin(2\pi y) + x^2 + y^2 + 1.$$

As far as the implementation of the MFD method is concerned, we consider the family of local scalar products given by [14]

$$M_E = \frac{1}{|E|} R\widetilde{\alpha}_E R^T + u_E C C^T, \tag{4.1}$$

where u_E is a nonnegative real parameter, and R and C are the matrices detailed below. In all our numerical experiments, we set $u_E = \mathrm{Tr}(\widetilde{K}_E)|E|$ to ensure the correct scaling with K and the element size.

The matrices R and C can be obtained as follows (cf. [14]). Let x_e^j and x_E^j for $j = 1,\dots,d$ be the jth component of the position vectors $\boldsymbol{x}_e$, the barycenter of the face e, and $\boldsymbol{x}_E$, the barycenter of the element E. Then,

$$\text{the } j\text{th column of } R \text{ is } \begin{pmatrix} |e_1|\big(x_{e_1}^j - x_E^j\big) \\ \vdots \\ |e_{m_E}|\big(x_{e_{m_E}}^j - x_E^j\big) \end{pmatrix} \in \mathbb{R}^{m_E} \quad \text{for } j = 1,\dots,d.$$

On its turn, C is the $m_E\times(m_E-d)$ matrix whose columns are a basis of the orthogonal complement in $\mathbb{R}^{m_E}$ of the vector space spanned by the linearly independent vectors

$$\boldsymbol{N}^j = \left(\widetilde{K}\widehat{\boldsymbol{x}}^j\right)^I \in \mathbb{R}^{m_E} \text{ for } j = 1,\dots,d,$$

where $\widehat{\boldsymbol{x}}^j$ is the unit vector along the direction of the jth coordinate axis. Note that the matrix R and the vectors $\boldsymbol{N}^j$ (and, thus, C) depend only on geometric quantities that can be easily calculated.

Remark 4.1. The derivation of (4.1) and of the above formulas defining the matrices R and C is beyond the scope of this paper and is thoroughly discussed in [14]. Here, we just note that the first term of the right-hand side of (4.1) is obtained from the local consistency condition (S2), while the other term ensures that M_E is a strictly positive definite matrix. In [11] it is shown that M_E is associated with a scalar product induced by a lifting operator, as required by our analysis, provided that the parameter u_E is above a threshold value. The existence of this threshold value was established through a theoretical argument that is only sufficient. Moreover, how

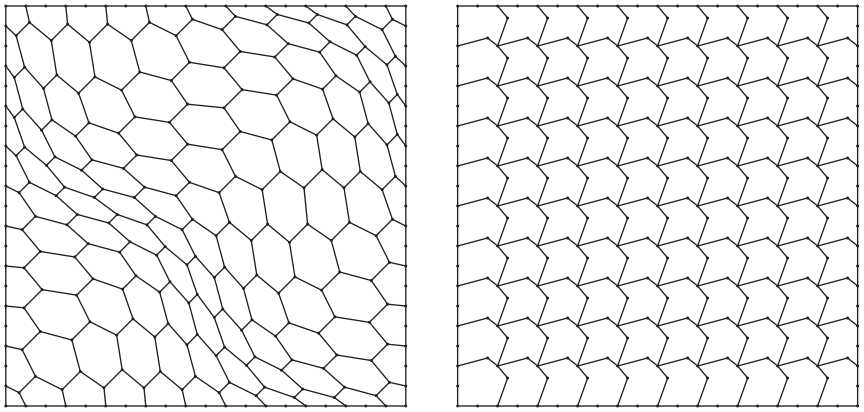

FIG. 4.1. *The base mesh of the mesh family $\mathcal{M}_1$ (left plot) and of the mesh family $\mathcal{M}_2$ (right plot) obtained with $n = 10$.*

to choose u_E in an "optimal" way is still an open issue. However, this aspect does not seem to be a critical point because, as shown in the aforementioned papers, the method is quite robust with respect to variations of u_E.

The performance of the mimetic finite difference method is investigated by evaluating the rate of convergence as the meshes are refined starting from a given base mesh. We consider two families of meshes, labeled by $\mathcal{M}_1$ and $\mathcal{M}_2$, whose construction and refinement algorithm is discussed below. These numerical experiments are carried out by using a C^{++} program based on a variant of P2MESH [7], a public domain library designed to manage data structures of unstructured meshes.

Each mesh of $\mathcal{M}_1$ is built by the following special dualization procedure of a "primal" mesh. The primal mesh is obtained by remapping the position (ξ, η) of the nodes of an $n \times n$ uniform grid as follows:

$$x = \xi + (1/10)\sin(2\pi\xi)\sin(2\pi\eta),$$
$$y = \eta + (1/10)\sin(2\pi\xi)\sin(2\pi\eta).$$

The corresponding mesh of $\mathcal{M}_1$ is then built from this primal mesh by first splitting each quadrilateral cell into two triangles and then connecting the barycenters of adjacent triangular cells by a straight line. The mesh construction is completed at the boundary Γ by connecting the barycenters of the triangular cells adjacent to Γ to the midpoints of boundary edges and to the boundary vertices of the primal mesh. The mesh corresponding to $n = 10$ is shown in the left plot of Figure 4.1; the successive refinements are generated by doubling n.

The meshes of $\mathcal{M}_2$ are obtained by filling the unit square with a suitably scaled nonconvex octagonal reference cell. The meshes are parametrized by the number of partitions n in each direction. The starting mesh is given by $n = 10$ and is shown in the right plot of Figure 4.1; the refined meshes are obtained by doubling this parameter.

Mesh data are listed in Table 4.1 for the refinement levels corresponding to the values of n reported in the first column. In the table, m_E is the number of mesh elements, m_e is the number of mesh edges, and h is the mesh size parameter.

The performance of the method is measured by means of the absolute and relative errors

$$\mathcal{E}_{\mathsf{abs}}(p_h) = \|p - p_h\|_{L^2(\Omega)}, \qquad \mathcal{E}_{\mathsf{rel}}(p_h) = \frac{\mathcal{E}_{\mathsf{abs}}(p_h)}{\|p\|_{L^2(\Omega)}}$$

TABLE 4.1
Mesh data for different refinement levels of the mesh families $\mathcal{M}_1$ and $\mathcal{M}_2$: m_E is the number of mesh elements, m_e is the number of mesh edges, and h is the mesh size parameter.

	Mesh $\mathcal{M}_1$			Mesh $\mathcal{M}_2$		
n	m_E	m_e	h	m_E	m_e	h
10	121	400	$9.135\,10^{-2}$	100	440	$7.762\,10^{-2}$
20	441	1400	$4.654\,10^{-2}$	400	1680	$3.881\,10^{-2}$
40	1681	5200	$2.346\,10^{-2}$	1600	6560	$1.941\,10^{-2}$
80	6561	20000	$1.175\,10^{-2}$	6400	25920	$9.703\,10^{-3}$
160	25921	78400	$5.880\,10^{-3}$	25600	103040	$4.851\,10^{-3}$
320	103041	310400	$2.940\,10^{-3}$	102400	410880	$2.426\,10^{-3}$

TABLE 4.2
Test case 1: *absolute and relative errors $\mathcal{E}_{abs}(p_h)$ and $\mathcal{E}_{rel}(p_h)$ in the L^2-norms and convergence rate on the meshes $\mathcal{M}_1$ and $\mathcal{M}_2$. The convergence rate is calculated using relative errors.*

	Mesh $\mathcal{M}_1$			Mesh $\mathcal{M}_2$		
n	$\mathcal{E}_{abs}(p_h)$	$\mathcal{E}_{rel}(p_h)$	Rate	$\mathcal{E}_{abs}(p_h)$	$\mathcal{E}_{rel}(p_h)$	Rate
10	$1.635\,10^{-1}$	$9.134\,10^{-2}$	$--$	$1.449\,10^{-1}$	$8.095\,10^{-2}$	$--$
20	$8.290\,10^{-2}$	$4.630\,10^{-2}$	1.007	$7.098\,10^{-2}$	$3.964\,10^{-2}$	1.029
40	$4.144\,10^{-2}$	$2.315\,10^{-2}$	1.012	$3.521\,10^{-2}$	$1.966\,10^{-2}$	1.011
80	$2.083\,10^{-2}$	$1.164\,10^{-2}$	0.995	$1.756\,10^{-2}$	$9.810\,10^{-3}$	1.003
160	$1.046\,10^{-2}$	$5.841\,10^{-3}$	0.995	$8.777\,10^{-3}$	$4.902\,10^{-3}$	1.000
320	$5.241\,10^{-3}$	$2.927\,10^{-3}$	0.996	$4.388\,10^{-3}$	$2.451\,10^{-3}$	1.000

TABLE 4.3
Test case 2: *absolute and relative errors $\mathcal{E}_{abs}(p_h)$ and $\mathcal{E}_{rel}(p_h)$ in the L^2-norms and convergence rate on the meshes $\mathcal{M}_1$ and $\mathcal{M}_2$. The convergence rate is calculated using relative errors.*

	Mesh $\mathcal{M}_1$			Mesh $\mathcal{M}_2$		
n	$\mathcal{E}_{abs}(p_h)$	$\mathcal{E}_{rel}(p_h)$	Rate	$\mathcal{E}_{abs}(p_h)$	$\mathcal{E}_{rel}(p_h)$	Rate
10	$1.684\,10^{-1}$	$9.408\,10^{-2}$	$--$	$1.426\,10^{-1}$	$7.964\,10^{-2}$	$--$
20	$8.490\,10^{-2}$	$4.742\,10^{-2}$	1.018	$7.061\,10^{-2}$	$3.944\,10^{-2}$	1.014
40	$4.218\,10^{-2}$	$2.356\,10^{-2}$	1.022	$3.515\,10^{-2}$	$1.963\,10^{-2}$	1.006
80	$2.115\,10^{-2}$	$1.182\,10^{-2}$	0.998	$1.755\,10^{-2}$	$9.805\,10^{-3}$	1.001
160	$1.061\,10^{-2}$	$5.928\,10^{-3}$	0.995	$8.775\,10^{-3}$	$4.901\,10^{-3}$	1.000
320	$5.320\,10^{-3}$	$2.971\,10^{-3}$	0.996	$4.387\,10^{-3}$	$2.450\,10^{-3}$	1.000

that are reported in Tables 4.2 and 4.3. The absolute and relative errors of the flux approximation $\boldsymbol{F}_h$, given by

$$\mathcal{E}_{abs}(\boldsymbol{F}_h) = \left\| \boldsymbol{F}^I - \boldsymbol{F}_h \right\|_{X_h}, \qquad \mathcal{E}_{rel}(\boldsymbol{F}_h) = \frac{\mathcal{E}_{abs}(\boldsymbol{F}_h)}{\left\| \boldsymbol{F}^I \right\|_{X_h}},$$

are reported in Tables 4.4 and 4.5.

We also consider the solution errors in the Q_h-norm, which are given by

$$\mathcal{E}_{abs,Q_h}(p_h) = \left\| p^I - p_h \right\|_{Q_h}, \qquad \mathcal{E}_{rel,Q_h}(p_h) = \frac{\mathcal{E}_{abs,Q_h}(p_h)}{\|p\|_{Q_h}}$$

and are reported in Tables 4.6 and 4.7. Convergence rates are calculated by using relative errors.

Notice that, for both mesh families $\mathcal{M}_1$ and $\mathcal{M}_2$, the parameter h reported in Table 4.1 is roughly halved when n is doubled. A thorough inspection of Tables 4.2

TABLE 4.4

Test case 1: *absolute and relative errors* $\mathcal{E}_{abs}(\boldsymbol{F}_h)$ *and* $\mathcal{E}_{rel}(\boldsymbol{F}_h)$ *in the* X_h*-norm and convergence rate on the meshes* $\mathcal{M}_1$ *and* $\mathcal{M}_2$*. The convergence rate is calculated using relative errors.*

	Mesh $\mathcal{M}_1$			Mesh $\mathcal{M}_2$		
n	$\mathcal{E}_{abs}(\boldsymbol{F}_h)$	$\mathcal{E}_{rel}(\boldsymbol{F}_h)$	Rate	$\mathcal{E}_{abs}(\boldsymbol{F}_h)$	$\mathcal{E}_{rel}(\boldsymbol{F}_h)$	Rate
10	1.200	$1.823\,10^{-1}$	$--$	1.697	$2.610\,10^{-1}$	$--$
20	$5.477\,10^{-1}$	$8.572\,10^{-2}$	1.118	$8.911\,10^{-1}$	$1.401\,10^{-1}$	0.897
40	$2.638\,10^{-1}$	$4.168\,10^{-2}$	1.052	$4.544\,10^{-1}$	$7.189\,10^{-2}$	0.962
80	$1.288\,10^{-1}$	$2.039\,10^{-2}$	1.034	$2.271\,10^{-1}$	$3.598\,10^{-2}$	0.998
160	$6.354\,10^{-2}$	$1.007\,10^{-2}$	1.018	$1.142\,10^{-1}$	$1.809\,10^{-2}$	0.991
320	$3.172\,10^{-2}$	$5.027\,10^{-3}$	1.002	$5.734\,10^{-2}$	$9.089\,10^{-3}$	0.993

TABLE 4.5

Test case 2: *absolute and relative errors* $\mathcal{E}_{abs}(\boldsymbol{F}_h)$ *and* $\mathcal{E}_{rel}(\boldsymbol{F}_h)$ *in the* X_h*-norm and convergence rate on the meshes* $\mathcal{M}_1$ *and* $\mathcal{M}_2$*. The convergence rate is calculated using relative errors.*

	Mesh $\mathcal{M}_1$			Mesh $\mathcal{M}_2$		
n	$\mathcal{E}_{abs}(\boldsymbol{F}_h)$	$\mathcal{E}_{rel}(\boldsymbol{F}_h)$	Rate	$\mathcal{E}_{abs}(\boldsymbol{F}_h)$	$\mathcal{E}_{rel}(\boldsymbol{F}_h)$	Rate
10	1.290	$2.726\,10^{-1}$	$--$	1.201	$2.536\,10^{-1}$	$--$
20	$6.705\,10^{-1}$	$1.416\,10^{-1}$	0.972	$5.922\,10^{-1}$	$1.251\,10^{-1}$	1.019
40	$3.368\,10^{-1}$	$7.115\,10^{-2}$	1.006	$2.942\,10^{-1}$	$6.216\,10^{-2}$	1.009
80	$1.683\,10^{-1}$	$3.555\,10^{-2}$	1.004	$1.469\,10^{-1}$	$3.103\,10^{-2}$	1.002
160	$8.409\,10^{-2}$	$1.776\,10^{-2}$	1.001	$7.337\,10^{-2}$	$1.550\,10^{-2}$	1.001
320	$4.208\,10^{-2}$	$8.889\,10^{-3}$	0.999	$3.664\,10^{-2}$	$7.741\,10^{-3}$	1.001

TABLE 4.6

Test case 1: *absolute and relative errors* $\mathcal{E}_{abs,Q_h}(p_h)$ *and* $\mathcal{E}_{rel,Q_h}(p_h)$ *in the* Q_h*-norm and convergence rate on the meshes* $\mathcal{M}_1$ *and* $\mathcal{M}_2$*. The convergence rate is calculated using relative errors.*

	Mesh $\mathcal{M}_1$			Mesh $\mathcal{M}_2$		
n	$\mathcal{E}_{abs,Q_h}(p_h)$	$\mathcal{E}_{rel,Q_h}(p_h)$	Rate	$\mathcal{E}_{abs,Q_h}(p_h)$	$\mathcal{E}_{rel,Q_h}(p_h)$	Rate
10	$5.491\,10^{-2}$	$3.069\,10^{-2}$	$--$	$3.241\,10^{-2}$	$1.813\,10^{-2}$	$--$
20	$1.930\,10^{-2}$	$1.078\,10^{-2}$	1.551	$9.396\,10^{-3}$	$5.250\,10^{-3}$	1.787
40	$5.026\,10^{-3}$	$2.807\,10^{-3}$	1.964	$2.439\,10^{-3}$	$1.362\,10^{-3}$	1.946
80	$1.340\,10^{-3}$	$7.483\,10^{-4}$	1.913	$6.203\,10^{-4}$	$3.464\,10^{-4}$	1.975
160	$3.409\,10^{-4}$	$1.904\,10^{-4}$	1.975	$1.561\,10^{-4}$	$8.720\,10^{-5}$	1.990
320	$8.587\,10^{-5}$	$4.796\,10^{-5}$	1.989	$3.907\,10^{-5}$	$2.182\,10^{-5}$	1.998

TABLE 4.7

Test case 2: *absolute and relative errors* $\mathcal{E}_{abs,Q_h}(p_h)$ *and* $\mathcal{E}_{rel,Q_h}(p_h)$ *in the* Q_h*-norm and convergence rate on the meshes* $\mathcal{M}_1$ *and* $\mathcal{M}_2$*. The convergence rate is calculated using relative errors.*

	Mesh $\mathcal{M}_1$			Mesh $\mathcal{M}_2$		
n	$\mathcal{E}_{abs,Q_h}(p_h)$	$\mathcal{E}_{rel,Q_h}(p_h)$	Rate	$\mathcal{E}_{abs,Q_h}(p_h)$	$\mathcal{E}_{rel,Q_h}(p_h)$	Rate
10	$6.032\,10^{-2}$	$3.373\,10^{-2}$	$--$	$2.474\,10^{-2}$	$1.383\,10^{-2}$	$--$
20	$2.210\,10^{-2}$	$1.235\,10^{-2}$	1.493	$7.463\,10^{-3}$	$4.170\,10^{-3}$	1.730
40	$5.944\,10^{-3}$	$3.320\,10^{-3}$	1.919	$2.018\,10^{-3}$	$1.127\,10^{-3}$	1.887
80	$1.556\,10^{-3}$	$8.688\,10^{-4}$	1.940	$5.207\,10^{-4}$	$2.908\,10^{-4}$	1.954
160	$3.935\,10^{-4}$	$2.198\,10^{-4}$	1.984	$1.325\,10^{-4}$	$7.399\,10^{-5}$	1.974
320	$9.953\,10^{-5}$	$5.559\,10^{-5}$	1.983	$3.309\,10^{-5}$	$1.848\,10^{-5}$	2.001

and 4.3 reveals that the numerical errors for p_h are approximately halved on each refinement. This implies that on both mesh families the solution errors in the L^2-norm are linearly decreasing with respect to h. This result is in accordance with the theoretical prediction of Theorem 3.9.

We cannot measure the approximation error $\|\boldsymbol{F} - R(\boldsymbol{F}_h)\|_{H(\mathsf{div},\Omega)}$, which is estimated by Theorem 3.12, as it contains the lifting operator R. Such error, though, is the sum of interpolation errors and the measurable approximation error $\|\boldsymbol{F}^I - \boldsymbol{F}_h\|_{X_h}$. Indeed,

$$\|\mathrm{div}(\boldsymbol{F} - R(\boldsymbol{F}_h))\|_{L^2(\Omega)} = \left\|f - f^I\right\|_{L^2(\Omega)}$$

and

$$\begin{aligned}\left\|\widetilde{\alpha}^{1/2}(\boldsymbol{F} - R(\boldsymbol{F}_h))\right\| &\le \left\|\widetilde{\alpha}^{1/2}\left(\boldsymbol{F} - R\left(\boldsymbol{F}^I\right)\right)\right\|_{L^2} + \left\|\widetilde{\alpha}^{1/2} R\left(\boldsymbol{F}^I - \boldsymbol{F}_h\right)\right\|_{L^2(\Omega)} \\ &= \left\|\widetilde{\alpha}^{1/2}\left(\boldsymbol{F} - R\left(\boldsymbol{F}^I\right)\right)\right\|_{L^2} + \left|\left|\left|\boldsymbol{F}^I - \boldsymbol{F}_h\right|\right|\right|_{X_h}.\end{aligned}$$

The interpolation errors are independent of the numerical method and are expected to decrease linearly with h, and the error in the X_h-norm is of order h as well of Tables 4.4 and 4.5.

Finally, the superconvergence of p_h to p^I is visible in Tables 4.6 and 4.7, as the numerical errors are divided by nearly 4 when h is halved. For test case 1, this is in agreement with the theoretical prediction of Theorem 3.11. As for test case 2, the requirements that the diffusion tensor is piecewise constant and the convection field belongs to V_h are not satisfied, and thus Theorem 3.11 does not apply. Nonetheless, the superconvergence of p_h to p^I is observed experimentally as shown in Table 4.7.

5. Conclusions. We extended the MFD method to general elliptic problems including convection and reaction terms. The method is formulated on unstructured polygonal and polyhedral meshes formed by generally shaped elements. Our a priori error analysis shows that the numerical approximation of the scalar solution and flux is optimal in the L^2-norm. Moreover, we proved that the mimetic elemental solution superconverges to the cell average of the exact solution. The present method is suitable to the diffusive regime of the model problem. It is reasonable to expect that numerical instabilities in the approximate solution arise in the convection-dominated regime until the mesh is fine enough. The design of mimetic discretizations free from instabilities in all regimes are under investigation and will be considered in future publications.

Acknowledgment. The authors thank Prof. F. Brezzi for his useful discussions and suggestions.

REFERENCES

[1] B. Andreianov, F. Boyer, and F. Hubert, *Discrete duality finite volume schemes for Leray-Lions type elliptic problems on general 2d meshes*, Numer. Methods Partial Differential Equations, 23 (2007), pp. 145–195.

[2] L. Beirao da Veiga and G. Manzini, *An a-posteriori error estimator for the mimetic finite difference approximation of elliptic problems*, Internat. J. Numer. Methods Engrg., 76 (2008), pp. 1696–1723.

[3] L. Beirão da Veiga and G. Manzini, *A higher-order formulation of the mimetic finite difference method*, SIAM J. Sci. Comput., 31 (2008), pp. 732–760.

[4] L. Beirão da Veiga, *A residual based error estimator for the mimetic finite difference method*, Numer. Math., 108 (2008), pp. 387–406.

[5] M. Berndt, K. Lipnikov, J. Moulton, and M. Shashkov, *Convergence of mimetic finite difference discretizations of the diffusion equation*, Numer. Math., 9 (2001), pp. 253–284.

[6] M. Berndt, K. Lipnikov, M. Shashkov, M. F. Wheeler, and I. Yotov, *Superconvergence of the velocity in mimetic finite difference methods on quadrilaterals*, SIAM J. Numer. Anal., 43 (2005), pp. 1728–1749.

[7] E. Bertolazzi and G. Manzini, *Algorithm* 817 *P2MESH: Generic object-oriented interface between* 2*-D unstructured meshes and FEM/FVM-based PDE solvers*, ACM Trans. Math. Software, 28 (2002), pp. 101–132.
[8] P. Bochev and J. M. Hyman, *Principles of mimetic discretizations of differential operators*, in Compatible Spatial Discretizations IMA Vol. 142, D. N. Arnold, P. B. Bochev, R. A. Lehoucq, R. A. Nicolaides, and M. Shashkov, eds., Math. Appl., Springer-Verlag, New York, 2006.
[9] S. Brenner and L. Scott, *The Mathematical Theory of Finite Element Methods*, Text Appl. Math. 15, Springer-Verlag, New York, 1994.
[10] F. Brezzi and M. Fortin, *Mixed and Hybrid Finite Element Methods*, Springer-Verlag, New York, 1991.
[11] F. Brezzi, K. Lipnikov, M. Shashkov, and V. Simoncini, *A new discretization methodology for diffusion problems on generalized polyhedral meshes*, Comput. Methods Appl. Mech. Engrg., 196 (2007), pp. 3682–3692.
[12] F. Brezzi, K. Lipnikov, and M. Shashkov, *Convergence of the mimetic finite difference method for diffusion problems on polyhedral meshes*, SIAM J. Numer. Anal., 43 (2005), pp. 1872–1896.
[13] F. Brezzi, K. Lipnikov, and M. Shashkov, *Convergence of mimetic finite difference methods for diffusion problems on polyhedral meshes with curved faces*, Math. Models Methods Appl. Sci., 16 (2006), pp. 275–298.
[14] F. Brezzi, K. Lipnikov, and V. Simoncini, *A family of mimetic finite difference methods on polygonal and polyhedral meshes*, Math. Models Methods Appl. Sci., 15 (2005), pp. 1533–1553.
[15] A. Cangiani and G. Manzini, *Flux reconstruction and pressure post-processing in mimetic finite difference methods*, Comput. Methods Appl. Mech. Engrg., 197 (2008), pp. 933–945.
[16] B. Cockburn, *An introduction to the discontinuous Galerkin method for convection-dominated problems*, in Advanced Numerical Approximation of Nonlinear Hyperbolic Equations (Cetraro, 1997), Lecture Notes in Math. 1697, Springer-Verlag, Berlin, 1998, pp. 151–268.
[17] Y. Coudière and G. Manzini, *The Discrete Duality Finite Volume Method for Convection-diffusion Problems*, SIAM J. Numer. Anal., to appear.
[18] Y. Coudière, J.-P. Vila, and P. Villedieu, *Convergence rate of a finite volume scheme for a two-dimensional diffusion convection problem*, M2AN Math. Model. Numer. Anal., 33 (1999), pp. 493–516.
[19] Y. Coudière and P. Villedieu, *Convergence of a finite volume scheme for the linear convection-diffusion equation on locally refined meshes*, M2AN Math. Model. Numer. Anal., 34 (2000), pp. 1123–1149.
[20] K. Domelevo and P. Omnes, *A finite volume method for the Laplace equation on almost arbitrary two-dimensional grids*, M2AN Math. Model. Numer. Anal., 39 (2005), pp. 1203–1249.
[21] J. J. Douglas and J. E. Roberts, *Mixed finite element methods for second order elliptic equations*, Mat. Appl. Comput., 1 (1982), pp. 91–103.
[22] J. J. Douglas and J. E. Roberts, *Global estimates for mixed methods for second order elliptic equations*, Math. Comp., 44 (1985), pp. 39–52.
[23] J. Droniou, *Error estimates for the convergence of a finite volume discretization of convection-diffusion equations*, J. Numer. Math., 11 (2003), pp. 1–32.
[24] R. Eymard, T. Gallouët, and R. Herbin, *Finite volume methods*, in Handbook for Numerical Analysis, Vol. VIII, P. Ciarlet and J. Lions, eds., North–Holland, Amsterdam, 2000, pp. 715–1022.
[25] R. Eymard, T. Gallouët, and R. Herbin, *A cell-centred finite volume approximation for anisotropic diffusion operators on unstructured meshes in any space dimension*, IMA J. Numer. Anal., 26 (2006), pp. 326–353.
[26] V. Gyrya and K. Lipnikov, *High-order mimetic finite difference method for diffusion problems on polygonal meshes*, J. Comput. Phys., 227 (2008), pp. 8841–8854.
[27] R. Herbin, *An error estimate for a finite volume scheme for a diffusion-convection problem on a triangular mesh*, Numer. Methods Partial Differential Equations, 11 (1995), pp. 165–173.
[28] F. Hermeline, *A finite volume method for the approximation of diffusion operators on distorted meshes*, J. Comput. Phys., 160 (2000), pp. 481–499.
[29] F. Hermeline, *Approximation of diffusion operators with discontinuous tensor coefficients on distorted meshes*, Comput. Methods Appl. Mech. Engrg., 192 (2003), pp. 1939–1959.
[30] P. Houston, C. Schwab, and E. Süli, *Discontinuous hp-finite element methods for advection-diffusion-reaction problems*, SIAM J. Numer. Anal., 39 (2002), pp. 2133–2163.
[31] J. M. Hyman and M. Shashkov, *Approximation of boundary conditions for mimetic finite-difference methods*, Comput. Math. Appl., 36 (1998), pp. 79–99.

[32] J. Hyman, J. Morel, M. Shashkov, and S. Steinberg, *Mimetic finite difference methods for diffusion equations*, Comput. Geosci., 6 (2002), pp. 333–352.
[33] J. Hyman, M. Shashkov, and M. Steinberg, *The numerical solution of diffusion problems in strongly heterogeneous non-isotropic materials*, J. Comput. Phys., 132 (1997), pp. 130–148.
[34] Y. Kuznetsov, K. Lipnikov, and M. Shashkov, *The mimetic finite difference method on polygonal meshes for diffusion-type problems*, Comput. Geosci., 8 (2005), pp. 301–324.
[35] R. D. Lazarov, L. Tobiska, and P. S. Vassilevski, *Streamline diffusion least-squares mixed finite element methods for convection-diffusion problems*, East-West J. Numer. Math., 5 (1997), pp. 249–264.
[36] K. Lipnikov, J. Morel, and M. Shashkov, *Mimetic finite difference methods for diffusion equations on non-orthogonal non-conformal meshes.*, J. Comput. Phys., 199 (2004), pp. 589–597.
[37] K. Lipnikov, M. Shashkov, and D. Svyatskiy, *The mimetic finite difference discretization of diffusion problem on unstructured polyhedral meshes*, J. Comput. Phys., 211 (2006), pp. 473–491.
[38] J. Morel, M. Hall, and M. Shaskov, *A local support-operators diffusion discretization scheme for hexahedral meshes*, J. Comput. Phys., 170 (2001), pp. 338–372.
[39] J. Morel, R. Roberts, and M. Shashkov, *A local support-operators diffusion discretization scheme for quadrilateral r - z meshes*, J. Comput. Phys., 144 (1998), pp. 17–51.
[40] K. W. Morton, *Numerical Solution of Convection-Diffusion Problems*, Chapman & Hall, London, 1996.
[41] H.-G. Roos, M. Stynes, and L. Tobiska, *Numerical Methods for Singularly Perturbed Differential Equations, Convection-Diffusion and Flow Problems*, Springer-Verlag, Berlin, 1996.
[42] J.-M. Thomas, *Mixed finite elements methods for convection-diffusion problems*, in Numerical Approximation of Partial Differential Equations (Madrid, 1985), North-Holland Math. Stud. 133, North–Holland, Amsterdam, 1987, pp. 241–250.